NATIONAL ADVISORY COMMITTEE FOR AERONAUTICS

TECHNICAL NOTE 2268

TESTS OF TWO-BLADE PROPELLERS IN THE LANGLEY 8-FOOT HIGH-SPEED TUNNEL TO DETERMINE THE EFFECT ON PROPELLER PERFORMANCE OF A MODIFICATION OF INBOARD PITCH DISTRIBUTION

By James B. Delano and Melvin M. Carmel

Langley Aeronautical Laboratory
Langley Field, Va.

Washington
February 1951

NATIONAL ADVISORY COMMITTEE FOR AERONAUTICS

TECHNICAL NOTE 2268

TESTS OF TWO-BLADE PROPELLERS IN THE LANGLEY 8-FOOT HIGH-SPEED TUNNEL TO DETERMINE THE EFFECT ON PROPELLER PERFORMANCE OF A MODIFICATION OF INBOARD PITCH DISTRIBUTION[1]

By James B. Delano and Melvin M. Carmel

SUMMARY

Tests of two propellers having two blades and differing only in the inboard pitch distribution were made in the Langley 8-foot high-speed tunnel to determine the effect of inboard pitch distribution on propeller performance. The inboard pitch distribution of the original propeller was designed for operation in the reduced velocity region ahead of an NACA cowling; the inboard pitch distribution of the modified propeller was increased for operation at or near free-stream velocities, such as would be obtained in a pusher installation. Tests were made at conditions covering climb, cruise, and high-speed operation. Wake surveys were taken behind the propellers in order to determine the distribution of thrust along the blades and to aid in the analysis of the results. Test results showed that the modified propeller was about 2.5 percent less efficient for a typical climb condition at all altitudes, 2 percent more efficient for one cruise condition, and 5 percent more efficient for high-speed operation. At the design high-speed condition, the modified propeller showed a 6-percent loss in efficiency due to compressibility; whereas the original propeller showed an 11-percent efficiency loss due to compressiblity. The lower compressibility loss for the modified propeller resulted from the fact that the inboard sections of this propeller could operate at increased thrust loading after compressibility losses had occurred at the outboard sections.

INTRODUCTION

A propeller incorporating some reduction of pitch over the inboard sections, in order to make it suitable for operation in the reduced velocity region ahead of an NACA cowling, was proposed for use in a pusher installation. Inasmuch as the inboard sections of the propeller

[1]Supersedes the recently declassified NACA ACR L4L20, "Tests of Two-Blade Propellers in the Langley 8-Foot High-Speed Tunnel to Determine the Effect on Propeller Performance of a Modification of Inboard Pitch Distribution" by James B. Delano and Melvin M. Carmel, Jan. 1945.

in the pusher installation operate at or near free-stream velocity, the suitability of the pitch distribution of the proposed design was questionable because calculations indicated that the inboard sections would operate at negative angles of attack. A modified propeller with a change only in pitch distribution was therefore designed to eliminate the calculated negative angles of attack for the inboard sections. Wind-tunnel tests of both propellers were made in order to evaluate the comparative merits of the two pitch distributions through the operational range of the propeller for the pusher installation.

The propeller problem was considered to be associated essentially with the effects of compressibility and propeller-body interference. Because of the limitations of size, type, speed, and power on available dynamometers at the Langley Laboratory, the time necessary to develop new counterrotating dynamometers, and the very small size of the propellers for an accurately simulated model of the pusher installation, it was agreed that the compressibility effects could more conveniently and accurately be determined with two-blade 4-foot-diameter propellers and the existing single-rotating tractor dynamometer at the Langley 8-foot high-speed tunnel. The propeller-body interference effects could more conveniently and accurately be studied in the Langley two-dimensional low-turbulence pressure tunnel as an extension of a program directed toward a study of the effects of shaft-housing-wing interference.

Power limitations of the available dynamometer in the Langley 8-foot high-speed tunnel precluded tests with a large number of blades, and the investigation of compressibility effects was therefore conducted with two-blade propellers at basic blade loadings corresponding to the actual operating blade loadings. In order to distinguish between compressibility effects produced by the inboard and tip sections, measurements of the thrust distribution by wake-survey methods were included.

SYMBOLS

C_T thrust coefficient

C_P power coefficient

J advance ratio

h blade thickness

b blade width

q dynamic pressure

M_o free-stream Mach number

M_t helical tip Mach number $\left(M_o\sqrt{1+\left(\frac{\pi}{J}\right)^2}\right)$

M_x section Mach number $\left(M_o\sqrt{1 + \left[\frac{\pi(r/R)}{J}\right]^2}\right)$

r blade-section radius or wake-station radius

R propeller tip radius

$\frac{dC_T}{d(r/R)}$ section thrust coefficient

η efficiency

β blade angle

ϕ_c corrected helix angle

D blade diameter

C_L lift coefficient

V local velocity

V_o free-stream velocity

APPARATUS AND METHODS

The tests were conducted in the Langley 8-foot high-speed tunnel. The propellers tested were 4 feet in diameter and consisted of two blades made of duralumin and constructed at the Langley Laboratory. The full-scale propeller originally proposed is an eight-blade dual-rotating pusher propeller, one blade of which is shown in figure 1. The modified propeller tested was similar to the original in the outboard sections and differed inboard only in a modification to the pitch distribution. NACA 16-series sections are used for both propellers investigated. The blade-form curves for the two propellers tested are shown in figure 2.

The model (fig. 3) was especially designed to have a high critical Mach number. The fuselage shape is the NACA form 111. (See reference 1.) The wing of the model extended through the tunnel walls and was fastened to the balance ring. The airfoil section is of 20-inch chord, is 9 percent thick, and has modified NACA 66-series sections. The critical Mach number of the model is much higher than the free-stream Mach numbers used in the present tests.

The forward 7.4 percent of the fuselage was used as a spinner containing the propeller hub. The propeller plane was located at 3.8 percent of the fuselage length to give a spinner diameter equal to 15 percent of the propeller diameter. A small gap between the propeller and the spinner surface was sealed by sponge rubber cemented to the blades so that no radial outflow from the spinner along the blades could occur.

The motor used to turn the propellers is of 10-inch diameter, is 30 inches long, and is housed within the fuselage. This motor was rated at 200 horsepower at 4900 rpm for 1/2 hour of operation. Power and speed variation of the motor was provided by a variable-frequency alternator.

The motor housing was mounted on ball bearings coaxial with the shaft and was prevented from rotating under the torque reaction by a hydraulic unit that transmitted the torque force to a balance which measured the torque. The propeller rotational speed was measured by a condenser tachometer mounted on the motor shaft.

The thrust was measured by the tunnel drag balance. The force indicated by the drag balance was the resultant force along the thrust axis. The propulsive thrust was therefore determined as the resultant force in the thrust direction with the propeller operating plus the drag of the model without the propeller.

A survey rake was suspended vertically from the top of the tunnel and was located about 18 inches behind the propeller plane in order to measure the distribution of thrust along the propeller. The lower end of the rake cleared the fuselage by approximately 0.5 inch. (See fig. 3.) The rake remained as part of the test installation for all runs. The rake installation was similar to an installation that had been shown in special tests to give average values of pressure fluctuations. Both total- and static-pressure measurements were taken and the section thrust coefficients were determined by the method of reference 2.

TESTS

Tests were conducted for eight blade angles and four values of the free-stream Mach number. The range of the tests is indicated in the following table:

Free-stream Mach number	Blade angle at 0.75 radius (deg)							
0.20	20	25	30	35	40	45	50	55
.30	--	--	30	35	--	--	--	--
.53	--	--	--	--	40	45	50	55
.62	--	--	--	--	--	45	50	55

The test procedure consisted in setting the blade angle at the desired value and raising the tunnel airspeed to the desired free-stream Mach number with the propeller windmilling. The range of advance ratio was then covered by increasing the propeller rotational speed while the free-stream Mach number was held constant. The range of advance ratio at a given free-stream Mach number was limited by either the propeller rotational speed or the power of the motor. For the low blade angles, the propeller rotational speed of 5000 rpm was the principal restriction; for the high blade angles, power limitation of the motor was the principal restriction. The data obtained, however, cover the climbing and high-speed conditions.

REDUCTION OF DATA

The force-test data have been reduced to the usual thrust and power coefficients and have been corrected for the equivalent free-stream velocity and for the buoyancy effect on model drag that occurs as a result of tunnel-wall constraint as explained in references 3 and 4.

The propeller characteristics are presented in figures 4 and 5. For each value of the free-stream Mach number, the propeller thrust coefficient, the power coefficient, and the efficiency are plotted against the advance ratio. A plot of the helical tip Mach number against advance ratio is included in each part of figures 4 and 5.

The thrust coefficient is determined from the propulsive thrust. The force actually measured during the tests was the net force in the drag direction, and the thrust was then determined as the net measured force plus the drag of the model without the propeller. The model was mounted with the thrust axis inclined 1.0° to the direction in which the force was actually measured. The cosine correction, however, is insignificant and was not applied.

The section thrust-coefficient curves (figs. 6 to 13) were computed from measurements of total-pressure changes in the wake of the propeller, inasmuch as the net thrust is given by the change of momentum in the ultimate wake. These curves are for the actual propellers tested, so that the propeller thrust coefficient may be obtained from the area under these curves. The thrust coefficients obtained from integration of the wake-section thrust coefficients are not presented in this paper.

The section thrust-coefficient curves are presented in figures 6 to 13. The values of the advance ratio are included in these figures. Corresponding force-test results may be obtained from figures 4 and 5. The value of the thrust coefficient obtained from integration of the curves of figures 6 to 13 does not necessarily agree with the thrust coefficients obtained from the force tests. The reason for this discrepency has been checked in another investigation (reference 5) and has been found to be caused by the assymmetrical wake pattern produced when the propeller thrust axis is at an angle of attack. The value of the wake surveys is not impaired, however, since these measurements are used comparatively to show the changes in thrust distribution for the two inboard-pitch distributions through the operating range of Mach number.

BASIS FOR COMPARISON OF PROPELLER CHARACTERISTICS

The actual propellers for the airplane consist of eight blades; whereas the propellers tested in the Langley 8-foot high-speed tunnel have two blades. The test results have been compared at conditions of equal free-stream Mach number, equal power loading per blade, and equal advance ratio. The advance ratio will be affected by the total disk loading; hence, comparisons will be altered. Inasmuch as only comparative results are required, the simplification adopted will not influence the conclusions. Representative full-scale operating conditions were assumed for the propellers and corresponding conditions were used for comparison of the results of the model propellers. The power coefficients for the operating conditions were assumed to be proportional to the number of blades; therefore, comparisons of the tunnel results are made at power coefficients one fourth the computed full-scale values for eight blades. The values assumed for the eight-blade propeller are as follows:

Number of blades	8
Diameter, feet	15
Propeller rotational speed, rpm	1050
Brake horsepower	3000
Altitude, feet	35,000
Density ratio	0.3098
High speed, miles per hour	410
Temperature, °F absolute	393.6
Speed of sound, miles per hour	663
Free-stream Mach number	0.62

The climb conditions were assumed to be the conditions for operation at constant airplane lift coefficient and at full power and propeller rotational speed. The advance ratio was found to have a value of 0.850 at sea level and to increase gradually to 1.165 at 20,000 feet. The Mach number for climb varied from 0.200 at sea level to 0.295 at 20,000 feet. The cruise condition was taken as 75 percent of full power at 35,000 feet, and the power was assumed to vary as the cube of the propeller rotational speed. From the preceding data the following operating conditions were computed:

Altitude	Attitude	M_o	J	C_P for full-scale eight-blade propeller	C_P for model two-blade propeller
0	Climb	0.200	0.850	0.170	0.042
20,000	Climb	.295	1.165	.316	.079
35,000	Cruise at 75-percent full power	.565	2.300	.550	.137
35,000	High speed at full power	.620	2.300	.550	.137

RESULTS AND DISCUSSION

Body interference.- The ultimate choice of a propeller for the pusher installation depends on the body interference that the propellers experience at the plane of rotation. The propellers tested were proposed for use on a pusher installation, although the tests of the model propellers in the Langley 8-foot high-speed tunnel were made on a tractor installation. (See fig. 3.) For application of these test data to the full-scale pusher installation, any difference in the distribution of velocity in the plane of the propellers should be considered. Surveys of axial velocity at the propeller plane were made at the same Mach numbers for which propeller force data were obtained. The ratio of the local velocity V, in the plane of the propeller, to the free-stream velocity V_o for the condition with the propeller removed is shown in figure 14. The velocity ratio V/V_o varies only slightly with Mach number; hence, one curve has been used to represent the velocity distribution. The velocity ratio at the surface of the spinner is about 0.90 and gradually increases to a value of 1.00 at the propeller-tip location. The radial distribution of velocity will not be very different at other peripheral locations, nor is it believed that, in the full-scale pusher installation, the velocity field will be very different if the low-drag characteristics of the installation are achieved.

Climb condition.- Propeller efficiencies for the climb condition at constant values of power coefficients at a free-stream Mach number of 0.20 are shown in figure 15. A value of 0.042 for the power coefficient C_P at an advance ratio of 0.85 represents climb condition at sea level. The propeller with the modified pitch distribution is about 2.5 percent less efficient than the original propeller. This difference in efficiency increases for higher values of advance ratio. For values of advance ratio less than 0.85, the difference in efficiency becomes less and the modified propeller may become more efficient than the original propeller at the lowest test values of the advance ratio.

For climb conditions at altitude, with the same engine power and propeller rotational speed, the power coefficient will increase because of the decrease in air density. For most airplanes, however, the maximum rate of climb at constant power output occurs at higher airspeeds with an increase in altitude. Under these conditions the advance ratio and free-stream Mach number will increase above the sea-level value. Figure 16(a) shows the change in operating condition with altitude when the airplane is assumed to fly at a constant value of the dynamic pressure q. The free-stream Mach number increases from 0.200 at sea level to 0.295 at 20,000 feet. Comparisons of data obtained at a Mach number of 0.20 (fig. 15) have been used, since only small differences are noted in the data between Mach numbers of 0.20 and 0.30 (figs. 4 and 5). The modified propeller is shown to be about 2 percent less efficient than the original propeller throughout the climb range (fig. 16(b)).

Corroboration of these force-test results is evident in the results of the wake surveys behind the propeller. The section thrust-coefficient curves obtained for both propellers for the climb condition are shown in figures 17 and 18. These curves were obtained by cross-plotting the basic data presented in figures 6 and 10 for values of the power coefficient bracketing the sea-level climb value of 0.042 at an advance ratio of 0.85 and 1.165. The point on the fuselage surface $\left(\frac{r}{R} = 0.34\right)$ at the plane of survey corresponds to the innermost root section $\left(\frac{r}{R} = 0.15\right)$ of the propeller, and the value of $\frac{r}{R} = 1.02$ corresponds to the tip of the propeller because of the spread of wake due to body interference. Integration of the sea-level curves for $C_P = 0.042$ and $J = 0.85$ (fig. 17) shows that the over-all thrust coefficient is 2 percent less for the modified propeller than for the original propeller. Integration of the 20,000-foot-altitude curves for $C_P = 0.079$ and $J = 1.165$ (fig. 18) shows that the over-all thrust coefficient is 5 percent less for the modified propeller than for the original propeller.

The most obvious and significant change noted from these results is the shift in the thrust loading of the modified propeller, especially at low or medium values of the power coefficient. The shift of thrust is toward the root sections, and the load on the outboard sections of the propeller is thus decreased. The loss in efficiency for the modified propeller is clearly evident. The thinner outboard sections that can carry more load efficiently are operating appreciably unloaded. The over-all distribution of load for the modified propeller at these conditions of operation is therefore far from optimum. The results presented in figure 17 show that, at higher power, the modified propeller becomes relatively more efficient than the original propeller.

Basic effect of differences in pitch distribution.- Figure 2 shows that the modified propeller has about 8° greater twist at the surface of the spinner than the original propeller; whereas the two propellers have the same twist distributions at the outboard sections. For propeller operation at the same blade angle measured at the 0.75 radius, the root sections of the modified propeller will be operating at higher angles of attack. If the root sections of the modified propeller are assumed to be unstalled, as analysis seems to indicate, the modified propeller will have to operate at a lower blade angle at the 0.75 radius than the original propeller in order to absorb the same power at the same advance ratio.

Under conditions of equal power coefficient and advance ratio for unstalled or subcritical-speed operation, the outboard sections of the modified propeller will generally produce less thrust than similar sections of the original propeller and the root sections will produce more thrust. The total effect is a shifting of the load on the blades toward the root sections of the modified propeller as is shown by these data. It is to be emphasized that local changes in the pitch distribution can, therefore, lead to significant changes in the entire load distribution (fig. 17).

High-speed condition.- The high-speed operating conditions for the propellers at an altitude of 35,000 feet are a free-stream Mach number of 0.62, an advance ratio of 2.30, and a power coefficient of 0.137. Propeller characteristics for constant power coefficients bracketing the design value are shown in figures 19, 20, and 21 for free-stream Mach numbers of 0.20, 0.53, and 0.62, respectively. Both propellers have the same efficiency at a free-stream Mach number of 0.53 for an advance ratio of 2.30, but the modified propeller is about 5 percent more efficient than the original propeller at a free-stream Mach number of 0.62 and thereby shows much less compressibility loss. This result is more clearly shown in figure 22 for the corresponding operating conditions. No compressibility loss for either propeller is shown at a free-stream Mach number of 0.53 ($M_t = 0.90$). At a free-stream Mach number of 0.62 ($M_t = 1.05$), the modified propeller shows a 6-percent compressibility loss; whereas the original propeller shows an 11-percent loss. The losses for the modified propeller, are about the same as those found for the NACA 4-(3)(08)-045 propeller which has a wider blade that utilizes thicker tip sections and lower design lift coefficients. At the same operating conditions the losses for the original propeller, however, are about the same as for the NACA 4-(3)(08)-03 propeller (reference 3), which has blades of about the same width but thicker tip sections and lower design lift coefficients.

The compressibility losses are clearly shown by the results of the wake surveys. Comparisons of the section thrust-coefficient curves for free-stream Mach numbers of 0.53 and 0.62 are shown in figures 23(a) and 23(b), respectively, for the design condition ($C_P = 0.137$ and $J = 2.30$) and for power coefficients bracketing the design value. At a free-stream Mach number of 0.53 apparently no compressibility loss occurs. At this Mach number, the tips of the propellers just begin to operate at speeds above the critical; hence, no large losses would be indicated. A comparison of these curves with curves for the climb condition shown in figure 17 shows that the thrust load on both propellers shifts toward the tips. The shift is due to the increase in the power and permits the outboard sections to operate at the higher, more efficient lift coefficients. Comparison of figures 8(a) and 8(b) with figures 12(a) and 12(b) shows that the same effect continues even at higher loadings - that is, at lower values of advance ratio.

The effect of compressibility is shown in the reduction of the peaks of the curves for two values of the power coefficient (fig. 23(b)). This compressibility loss is more evident in figure 24, which gives the results for Mach numbers of 0.53 and 0.62. Losses in thrust loading are shown for both blades outboard of the 0.67-radius wake station. As was expected, the greatest losses occurred for the center sections, which were the most highly loaded at a Mach number of 0.53. Comparison of the integrated thrust coefficients shows an 8-percent loss in thrust for the modified propeller and an 18-percent loss for the original propeller; whereas the force-test results show efficiency losses of only 6 percent and 11 percent, respectively.

The increase in thrust coefficient produced by the inboard sections when the free-stream Mach number changes from 0.53 to 0.62 is particularly significant. This increase is to be expected for sections operating below their critical speeds. When the outboard sections operate beyond their critical speeds, the angle for zero lift of a section changes and, for operation at a given blade angle, the section angle of attack is reduced. The thrust coefficient and the power coefficient also are reduced. In order for the propeller to operate at the same power coefficient, the angle of attack must be increased; such an increase causes a corresponding increment in thrust for the inboard sections. Figure 24 shows that the increase in thrust for the inboard sections of the modified propeller is greater than the increase for the inboard sections of the original propeller and indicates that the inboard sections for the modified propeller are operating on a more favorable part of the lift curve. This result is of further significance because it indicates that, when the outboard sections suffer compressibility losses, the use of inboard sections capable of operating at greater loads will reduce the over-all propeller losses. The use of good propeller sections having high critical speed in the inboard sections is indicated. The superiority of the modified blade is thus clearly evident for the high-speed operating condition. Figure 21 indicates that the modified propeller will also be more efficient than the original propeller at higher power coefficients for almost all values of the advance ratio. Operation at higher tip speeds ($J < 2.3$) may show an even greater efficiency for the modified propeller.

The better performance of the modified propellers is also indicated by plots showing the section blade angle and corrected helix angles for the high-speed operating condition. This result is shown in figure 25 for a Mach number of 0.62. Similar curves could be obtained for a Mach number of 0.53, except that the section Mach number would be lower over the entire blade, varying from 0.49 at $\frac{r}{R} = 0.15$ to 0.90 at the tip (85.5 percent of values at $M_o = 0.62$). The pitch distributions for both propellers are closer to the uniform distribution at the high-speed condition than at the climb condition. All sections of the modified propeller operate at positive angles of attack at high-speed conditions; whereas the root sections of the original propeller operate at negative angles of attack and negative lift. Most of the sections of the modified propeller operate at slightly lower angles of attack $\left(\text{outboard of } \frac{r}{R} = 0.45\right)$ and would therefore be expected to show lower compressibility losses since the section speeds for these sections are above the critical value.

Cruise condition.- The cruise condition at an altitude of 35,000 feet is assumed to be 75 percent of full power. The engine power for this condition is assumed to be proportional to the cube of the propeller rotational speed and, in order to permit computation of the advance ratio, airplane velocity is assumed to be proportional to the cube root of the engine power. For these assumptions, the power coefficient and advance ratio are the same as the values obtained for the high-speed condition ($C_P = 0.137$ and $J = 2.30$). The Mach number is computed to be 0.565. The results showing the compressibility losses for the high-speed condition (fig. 22) can then be used to show the cruise performance. At a Mach number of 0.565, the modified propeller is about 2 percent more efficient than the original propeller. For cruise at power different from that assumed, the modified blade will be more efficient if the free-stream Mach number is between 0.53 and 0.62. It is important to note that both the high-speed and cruising operations for the propellers are at tip speeds greater than the critical tip speed for the propellers. The efficiency of the modified propeller for this condition thus indicates significant increased range performance for operation at Mach numbers higher than 0.53.

Improvement of propeller design.- The analysis of the results indicates that, for the cruise operation, both propellers were operating at or slightly above the critical tip Mach number; whereas for the high-speed operation both propellers were operating well beyond the critical tip Mach number ($M_t = 1.05$). This difference indicates that the cruise performance would be improved if the high-speed performance could be improved. The importance of utilizing the correct pitch distribution is evident from a comparison of the relative losses in efficiency at a tip Mach number of 1.05. The pitch distribution of the modified blade allowed this blade to operate at the high-speed condition with the outboard sections at lower values of lift coefficient and the inboard sections at higher values. This shift in distribution of lift gives a distribution of load along the blade that is desirable. In both cases, a better distribution of load along the blades results at this condition. An analysis of these results indicates that, if a propeller is to be designed to operate more efficiently at a free-stream Mach number of 0.62, one of two methods may be used. One method is evident from figures 4(d) and 5(d) - namely, designing the propeller to operate at higher advance ratios and thus at lower tip speeds. The other method - increasing the solidity and reducing the operating lift coefficient in order to maintain the same load at high speeds - will increase the critical speed of the sections. These two possibilities are also evident from the results of reference 3. If the method of designing propellers to operate at the higher advance ratios is employed, the correct pitch distribution must be used. The method in which the blade solidity is increased and the operating lift coefficient is decreased will cause an increase of propeller weight. The method of operating at higher advance ratios requires operating at lower propeller rotational speed for a given propeller diameter or, if the diameter is decreased and the propeller rotational speed is the same, wider blades will probably have to be used. A combination of these methods may be used to produce a propeller even closer to the optimum for the high-speed condition than the design tested.

CONCLUSIONS

Tests were made of two propellers differing only in the pitch distribution of the inboard sections to be used on a pusher installation. The original propeller was designed for operation in front of a cowling; whereas the modified propeller incorporated an increase in pitch distribution along the inboard sections for operation at or near free-stream velocities. The following conclusions for the conditions analyzed were obtained for the two-blade model propellers:

1. The modified propeller is 2.5 percent less efficient than the original propeller for climb at all altitudes, 2 percent more efficient for cruise at 75 percent of full power, and 5 percent more efficient for the high-speed condition.

2. For the design high-speed condition, the modified propeller shows a loss of 6 percent in efficiency due to compressibility and the original propeller shows a corresponding loss of 11 percent. The lower compressibility loss for the modified propeller resulted from the fact that the inboard sections of this propeller could operate at increased thrust loading after compressibility losses had occurred at the outboard sections.

3. These results indicate that the compressibility loss for a propeller may be reduced by the use of inboard sections that are capable of operating at greater loadings after the outboard sections reach their critical speed.

4. In order to increase the high-speed performance of these propellers, consideration must be given to the reduction of tip speed and the increase in blade width or to the use of wider blades operating at lower lift coefficient.

Langley Aeronautical Laboratory
National Advisory Committee for Aeronautics
Langley Field, Va., November 18, 1944

REFERENCES

1. Abbott, Ira H.: Fuselage-Drag Tests in the Variable-Density Wind Tunnel: Streamline Bodies of Revolution, Fineness Ratio of 5. NACA TN 614, 1937.

2. Baals, Donald D., and Mourhess, Mary J.: Numerical Evaluation of the Wake-Survey Equations for Subsonic Flow Including the Effect of Energy Addition. NACA ARR L5H27, 1945.

3. Stack, John, Draley, Eugene C., Delano, James B., and Feldman, Lewis: Investigation of the NACA 4-(3)(08)-03 and NACA 4-(3)(08)-045 Two-Blade Propellers at Forward Mach Numbers to 0.725 to Determine the Effects of Compressibility and Solidity on Performance. NACA Rep. 999, 1950.

4. Fage, A., Lock, C. N. H., Bateman, H., and Williams, D. H.: Experiments with a Family of Airscrews Including Effect of Tractor and Pusher Bodies. Part II - Experiments on Airscrews with Tractor and Pusher Bodies. R. & M. No. 830, British A.R.C., 1922.

5. Pendley, Robert E.: Effect of Propeller-Axis Angle of Attack on Thrust Distribution over the Propeller Disk in Relation to Wake-Survey Measurements of Thrust. NACA ARR L5J02b, 1945.

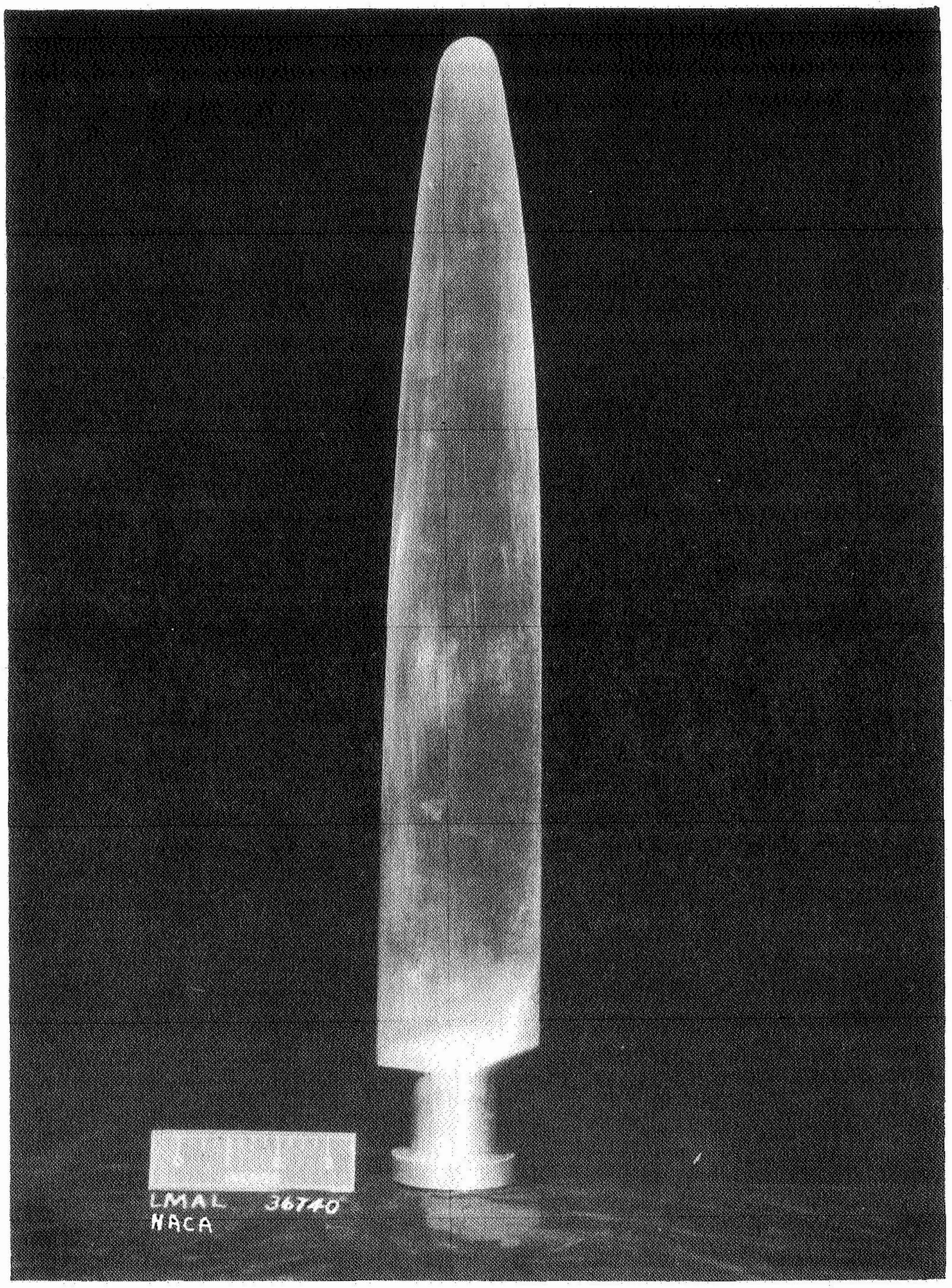

Figure 1.- Test blade.

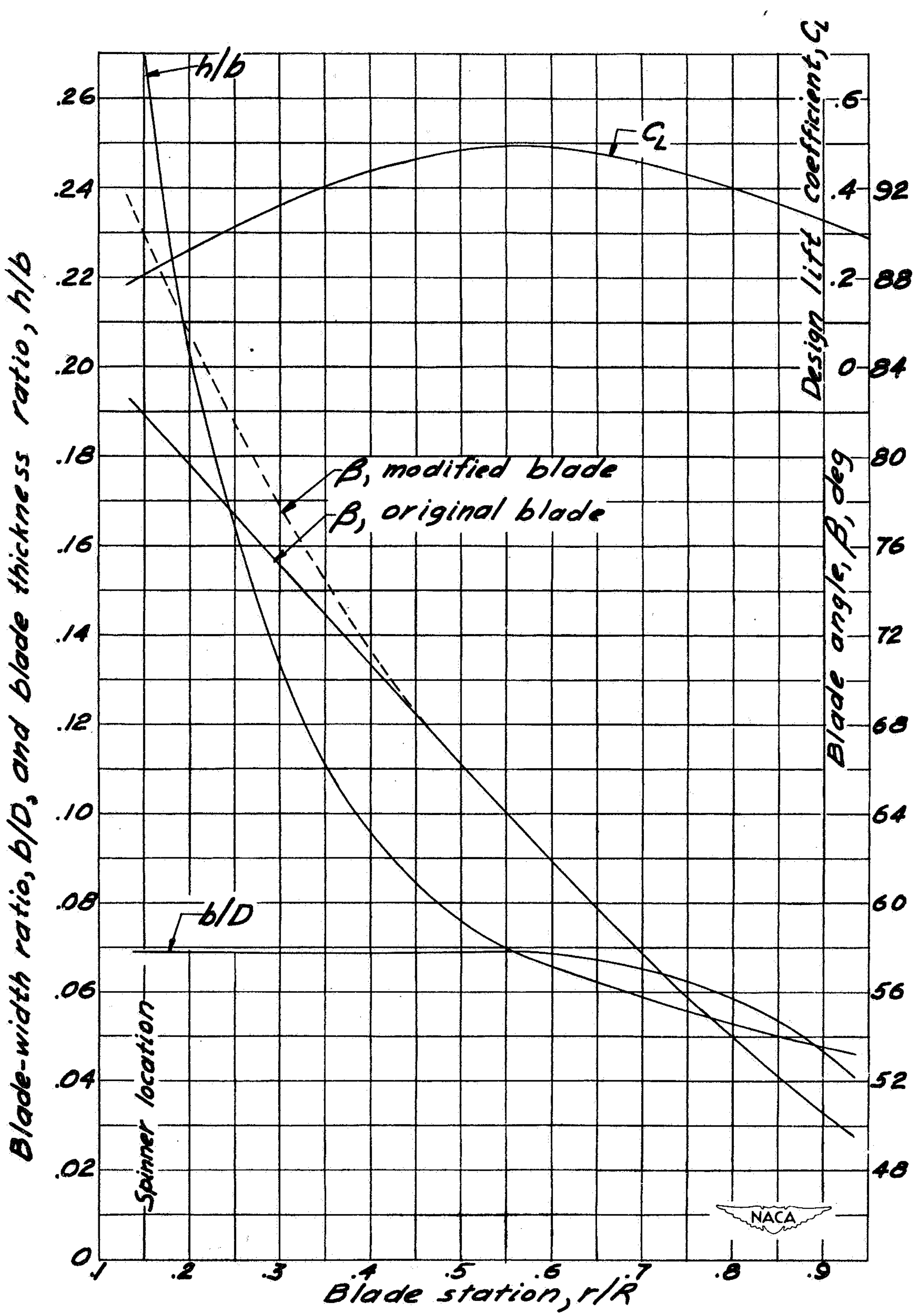

Figure 2.- Blade-form curves for the propellers tested.

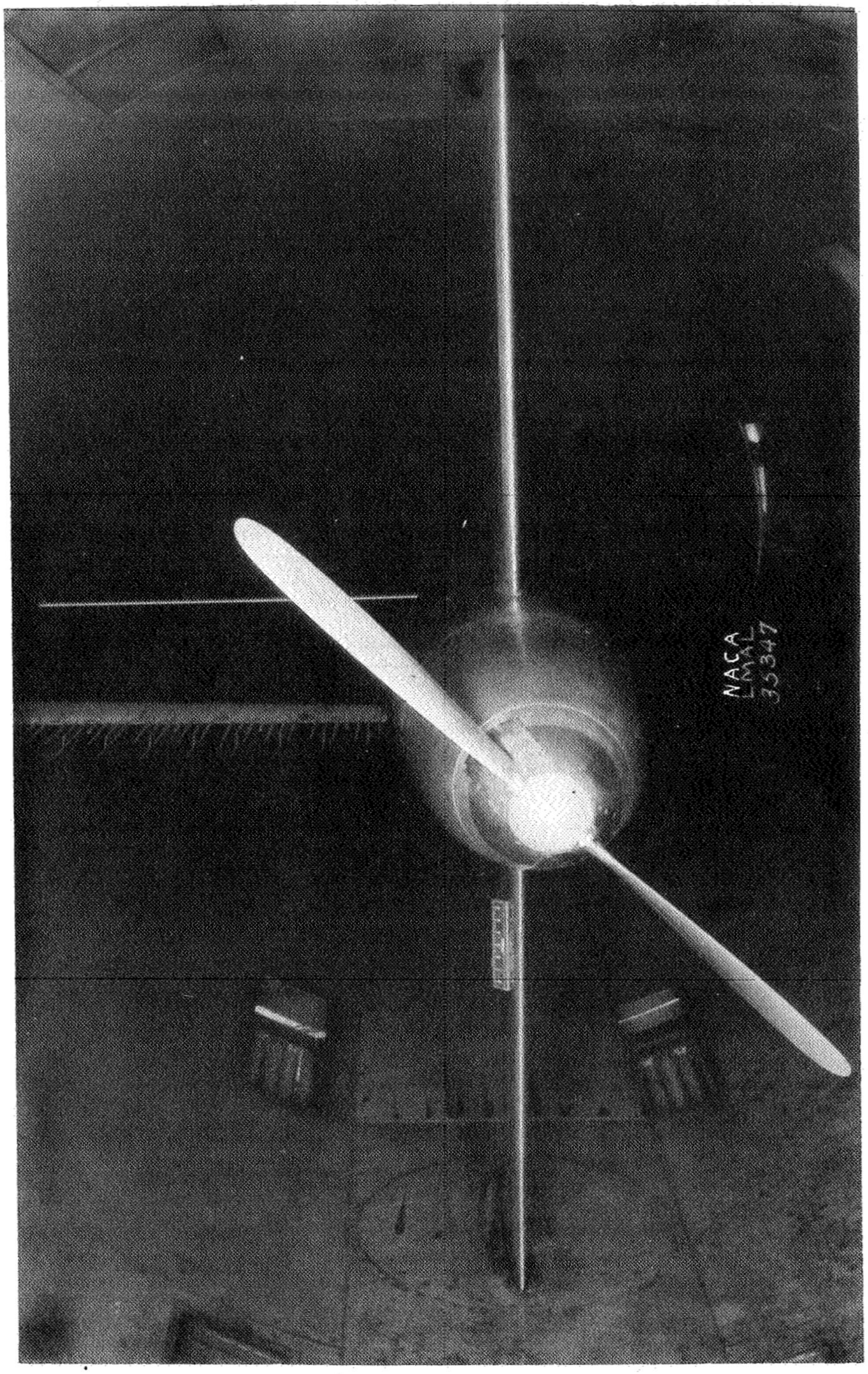

Figure 3.- Propeller setup in the Langley 8-foot high-speed tunnel.

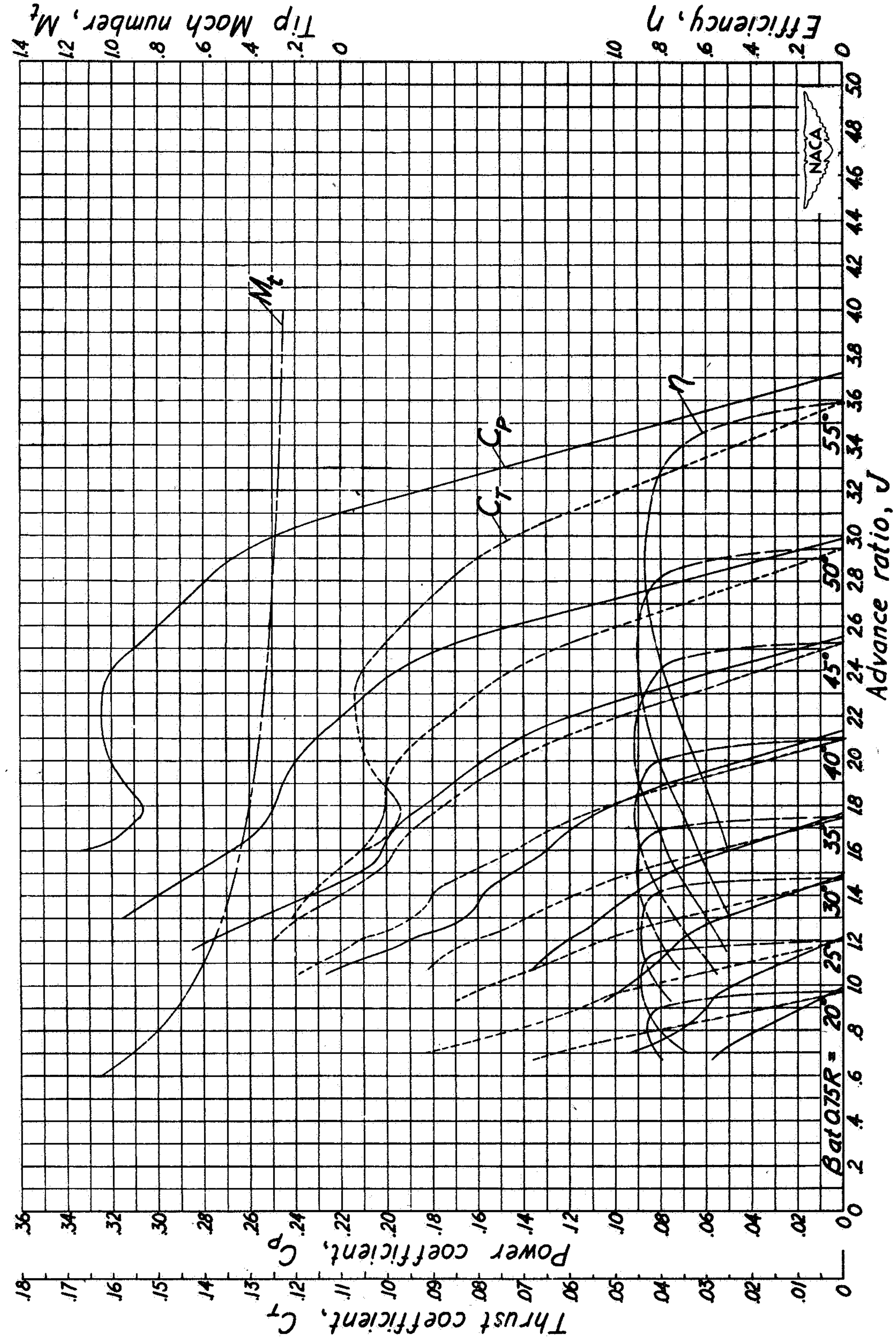

(a) $M_0 = 0.20$.

Figure 4.- Characteristics for original propeller.

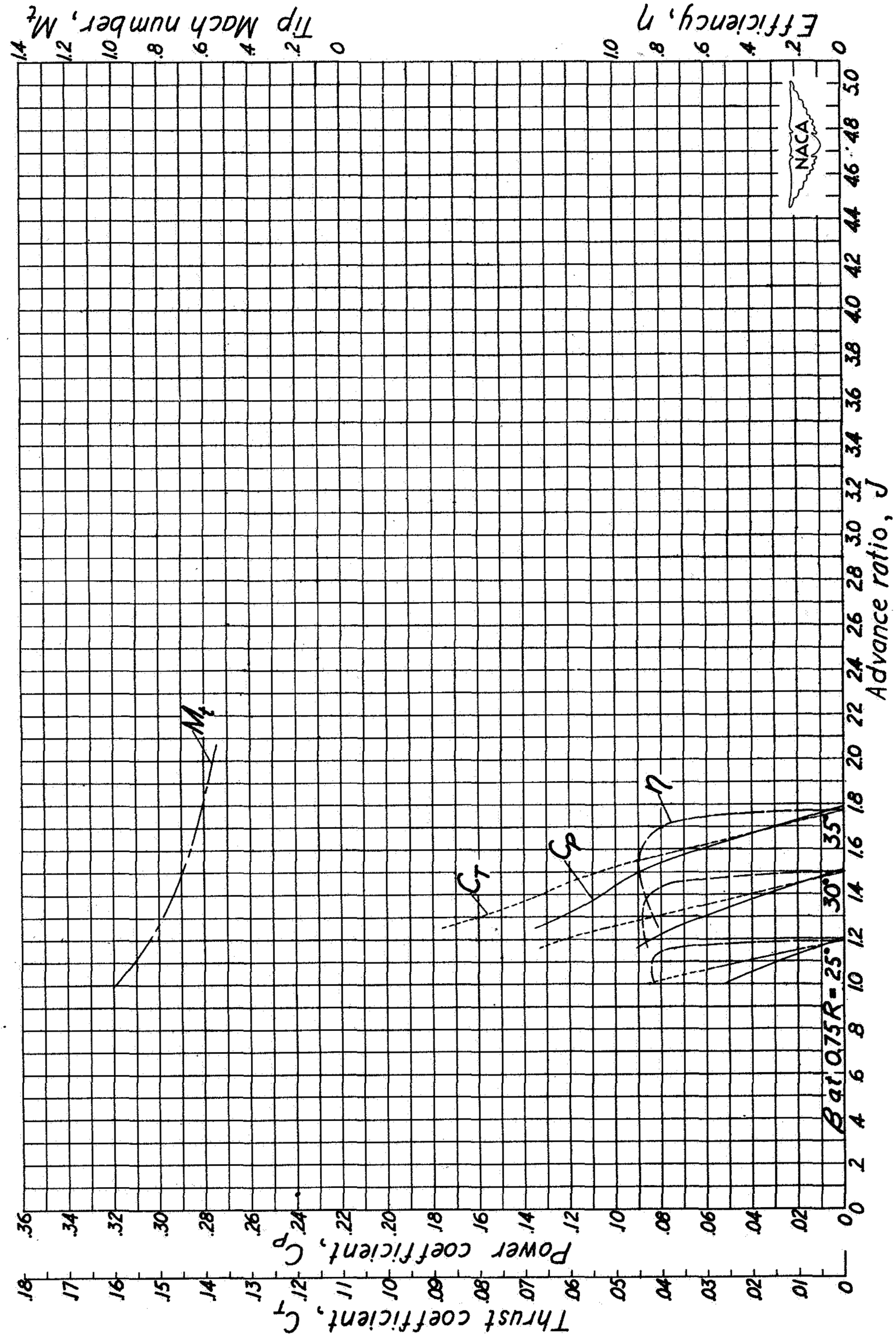

(b) $M_0 = 0.30$.

Figure 4.- Continued.

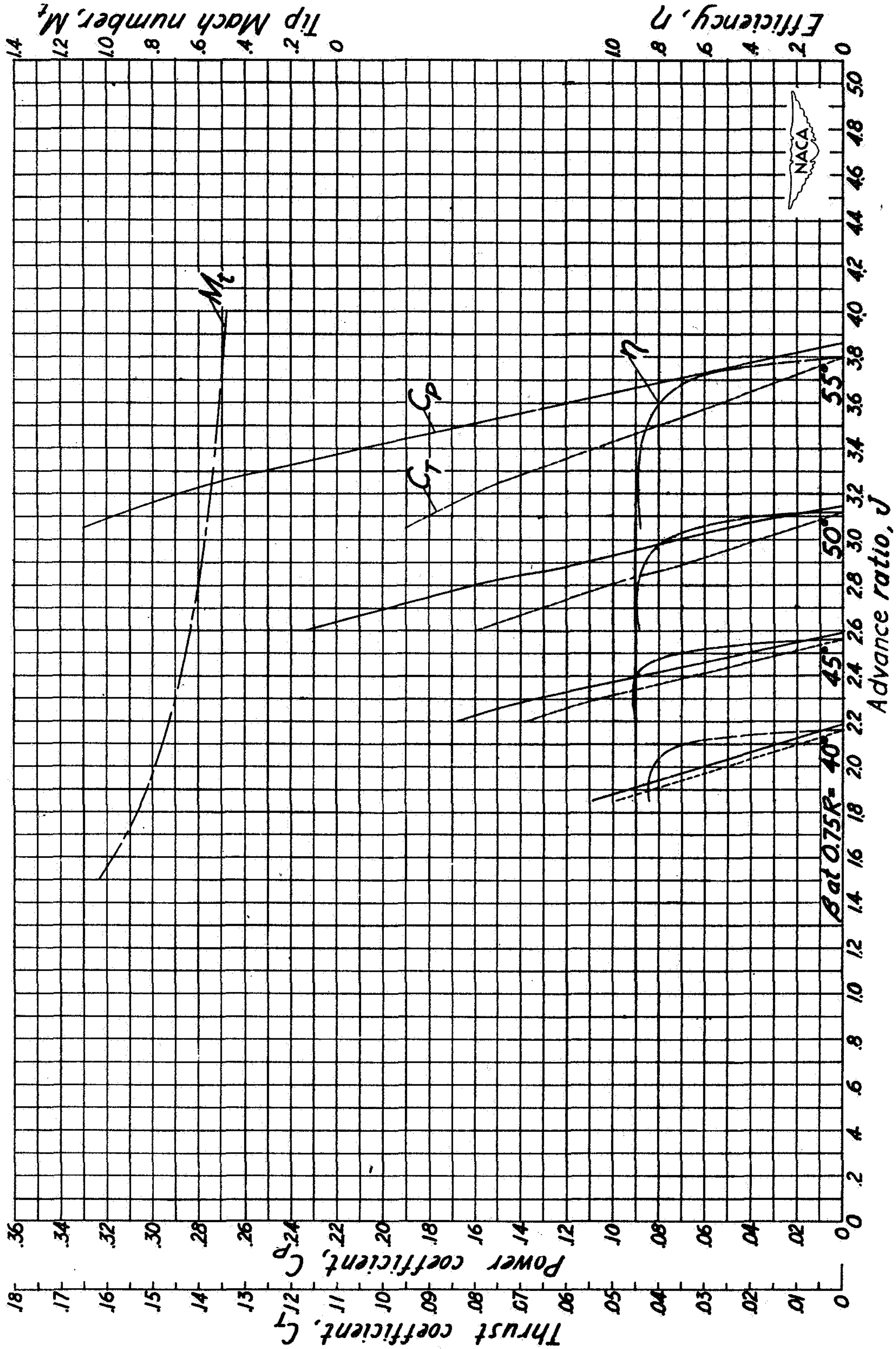

(c) $M_o = 0.53$.

Figure 4.- Continued.

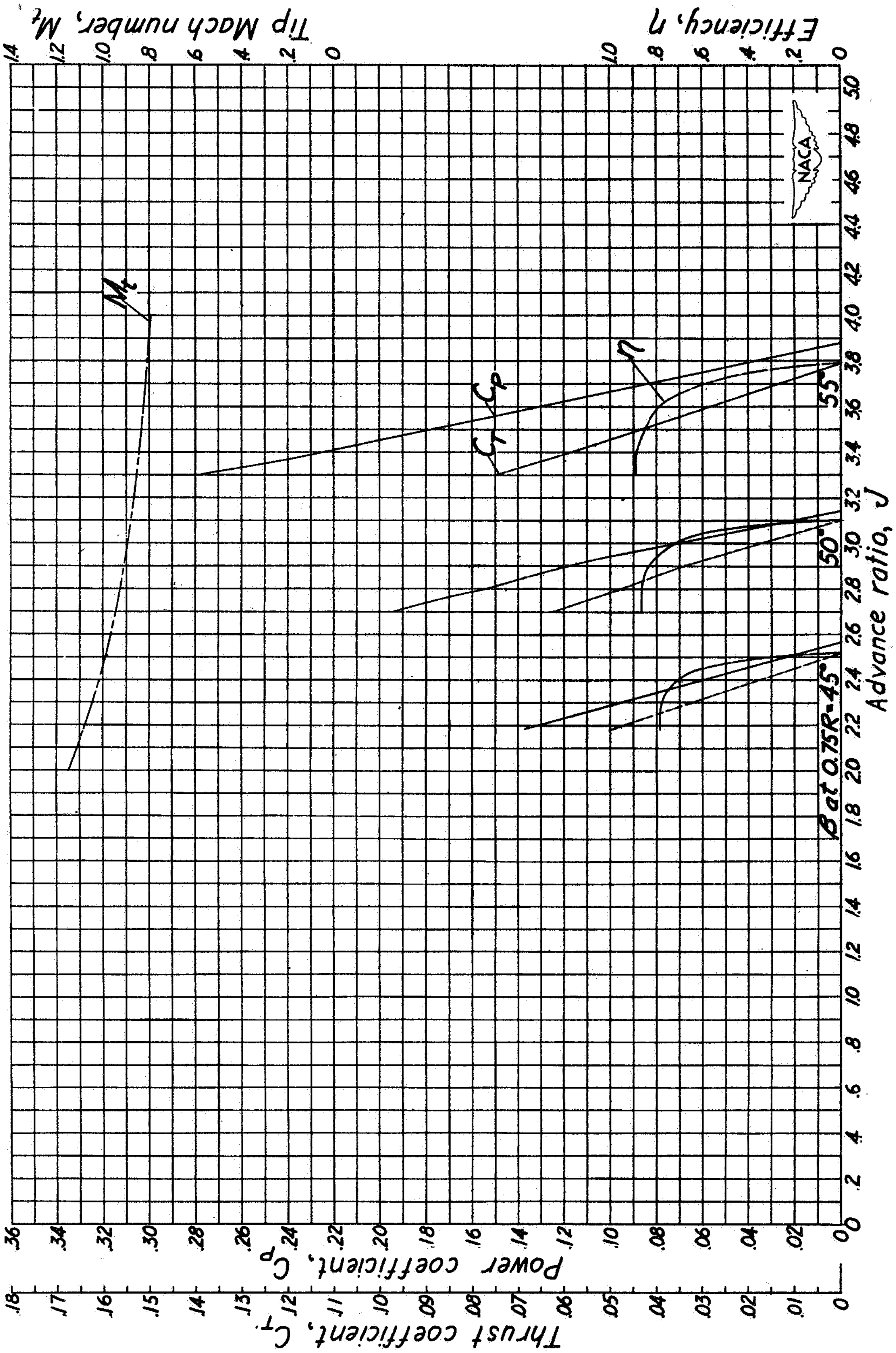

(d) $M_o = 0.62$.

Figure 4.- Concluded.

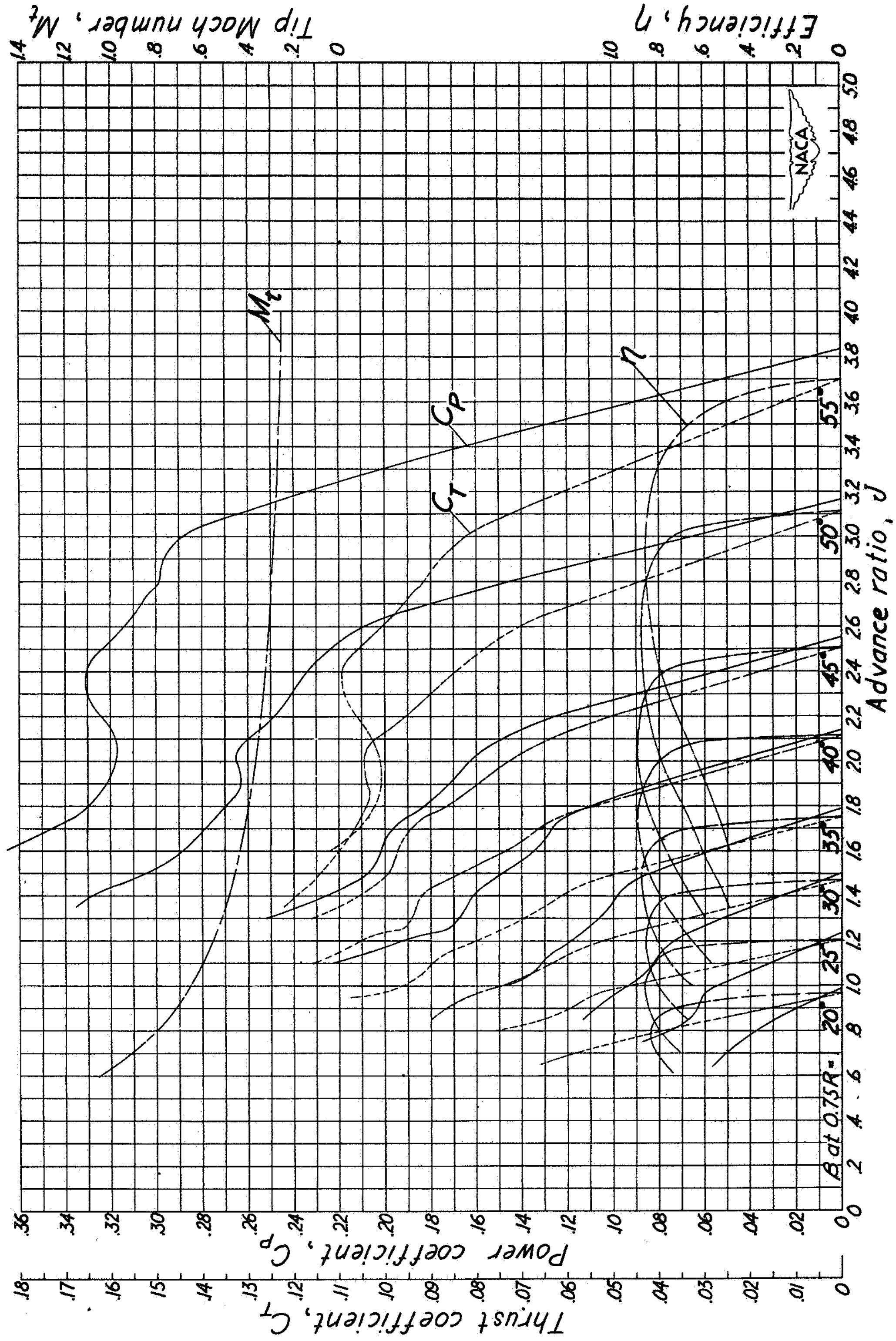

(a) $M_o = 0.20$.

Figure 5.- Characteristics for modified propeller.

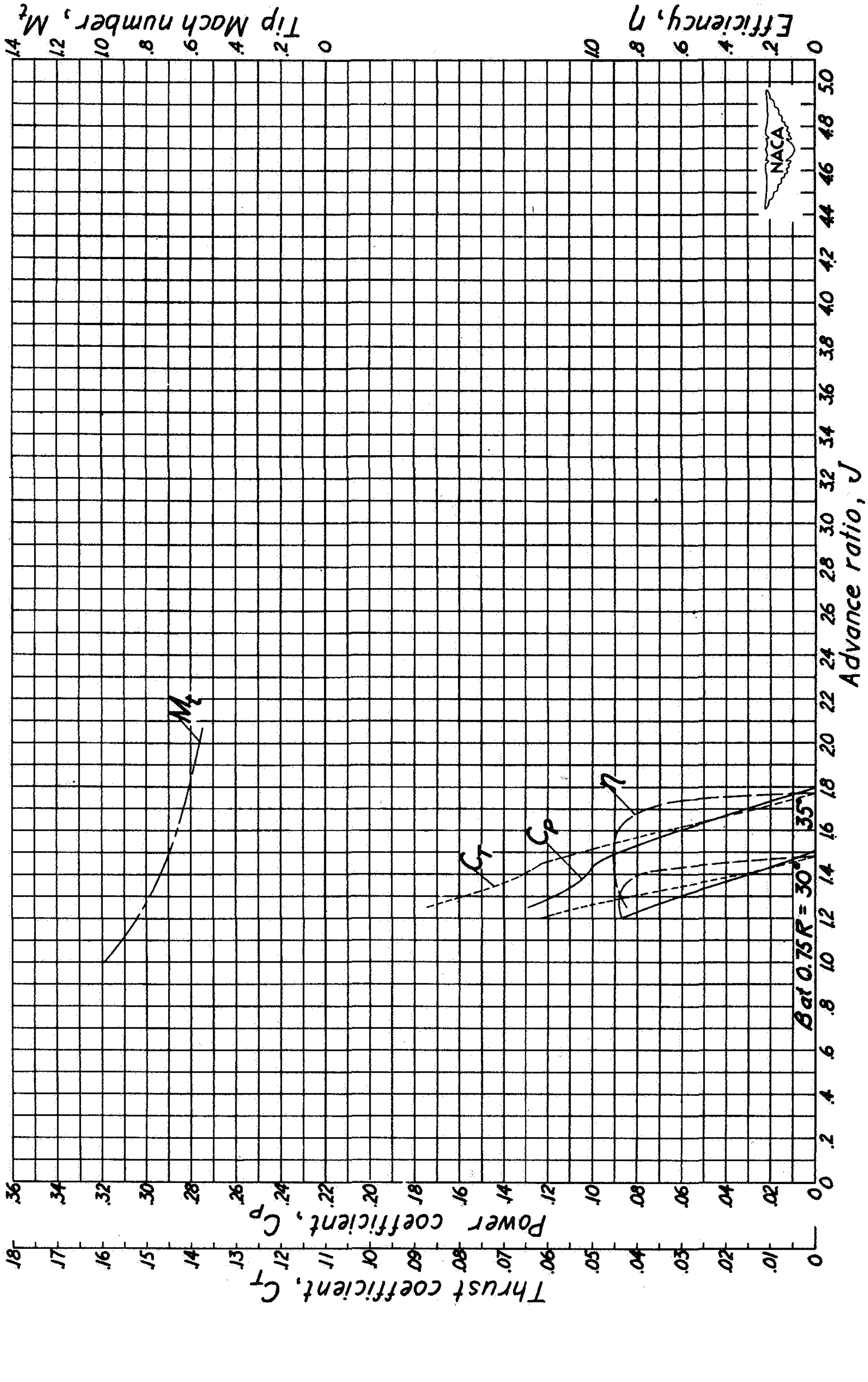

(b) $M_0 = 0.30$.

Figure 5.- Continued.

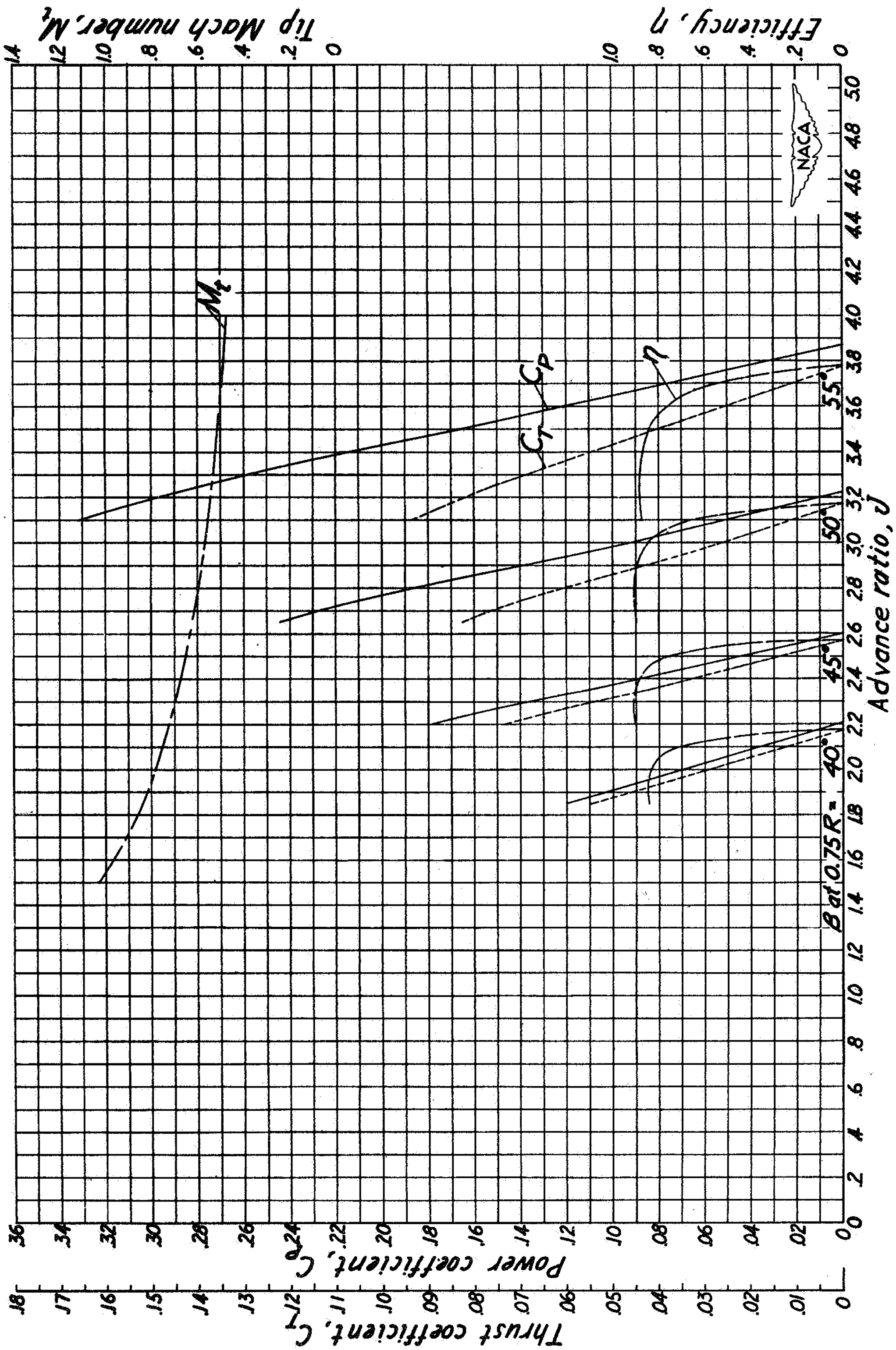

(c) $M_o = 0.53$.

Figure 5.- Continued.

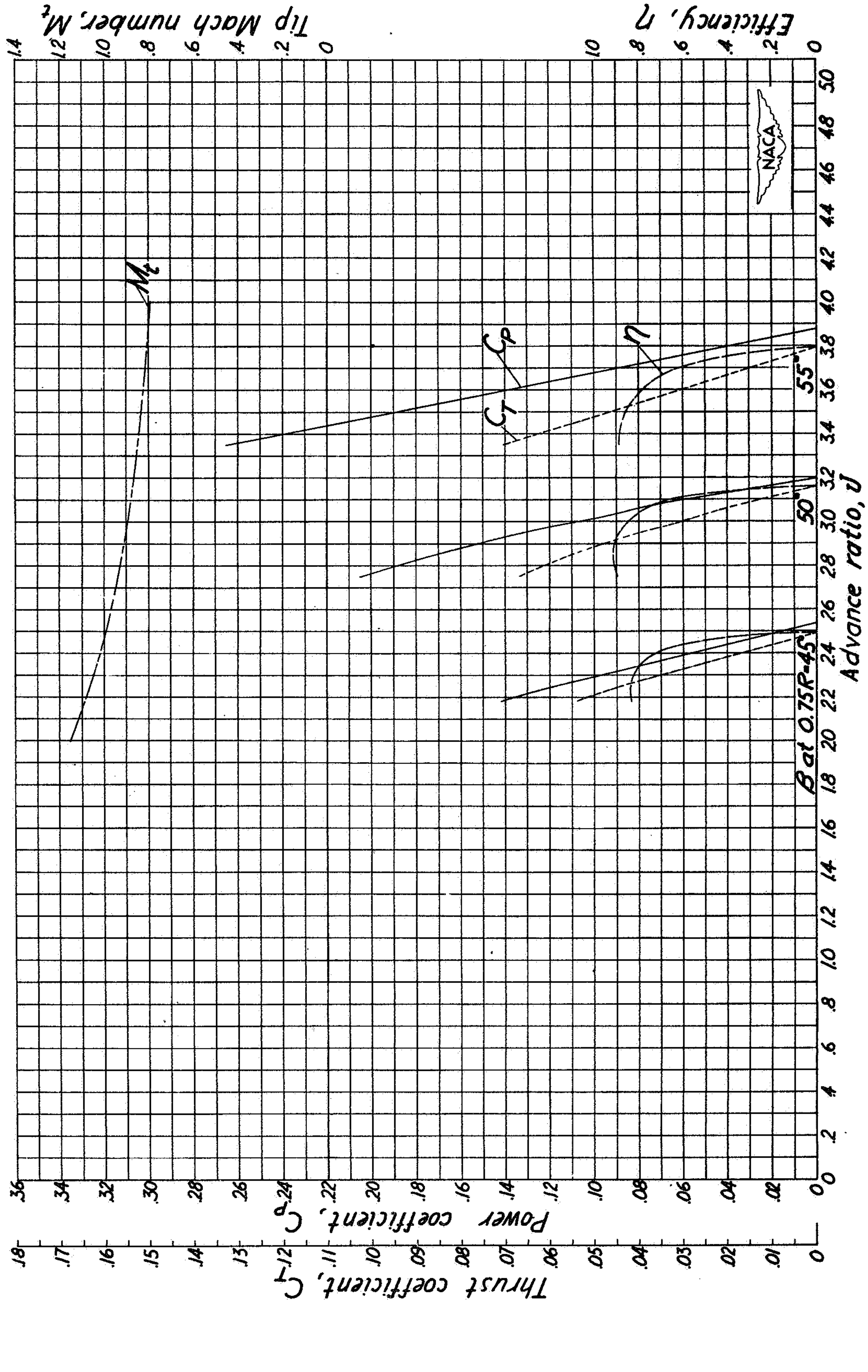

(d) $M_o = 0.62$.

Figure 5.- Concluded.

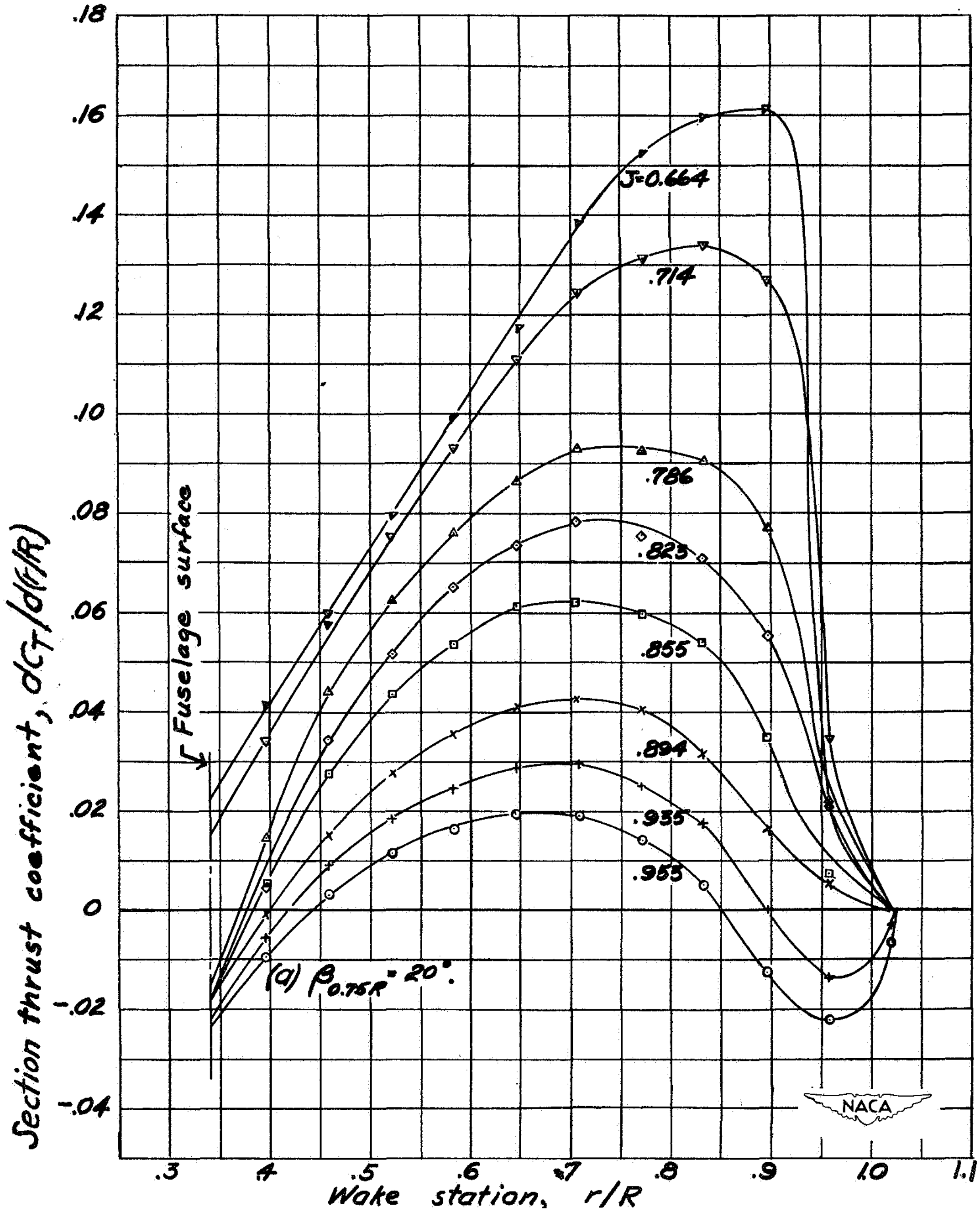

Figure 6.- Section thrust-coefficient curves for the original propeller. $M_o = 0.20$.

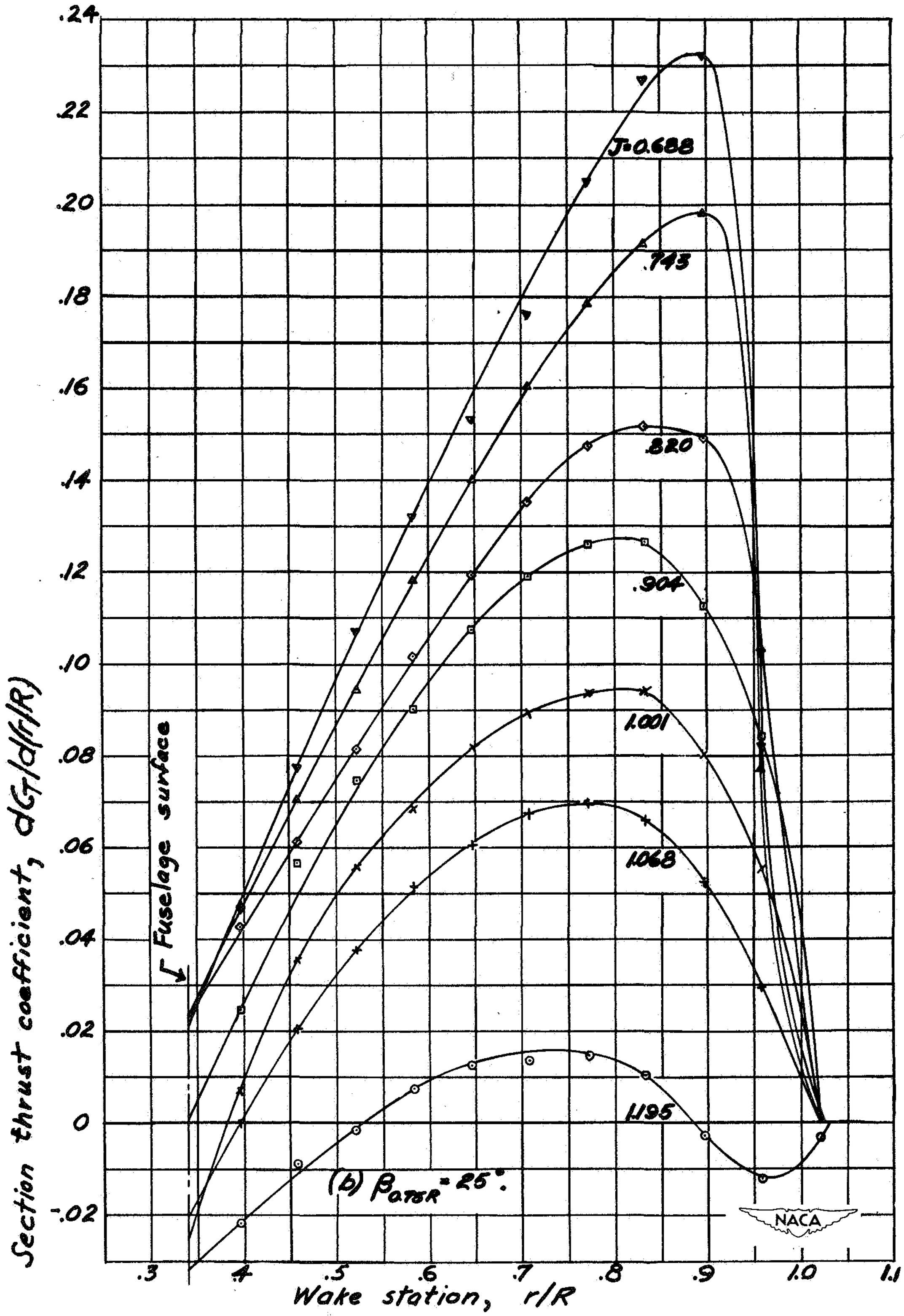

Figure 6.- Continued.

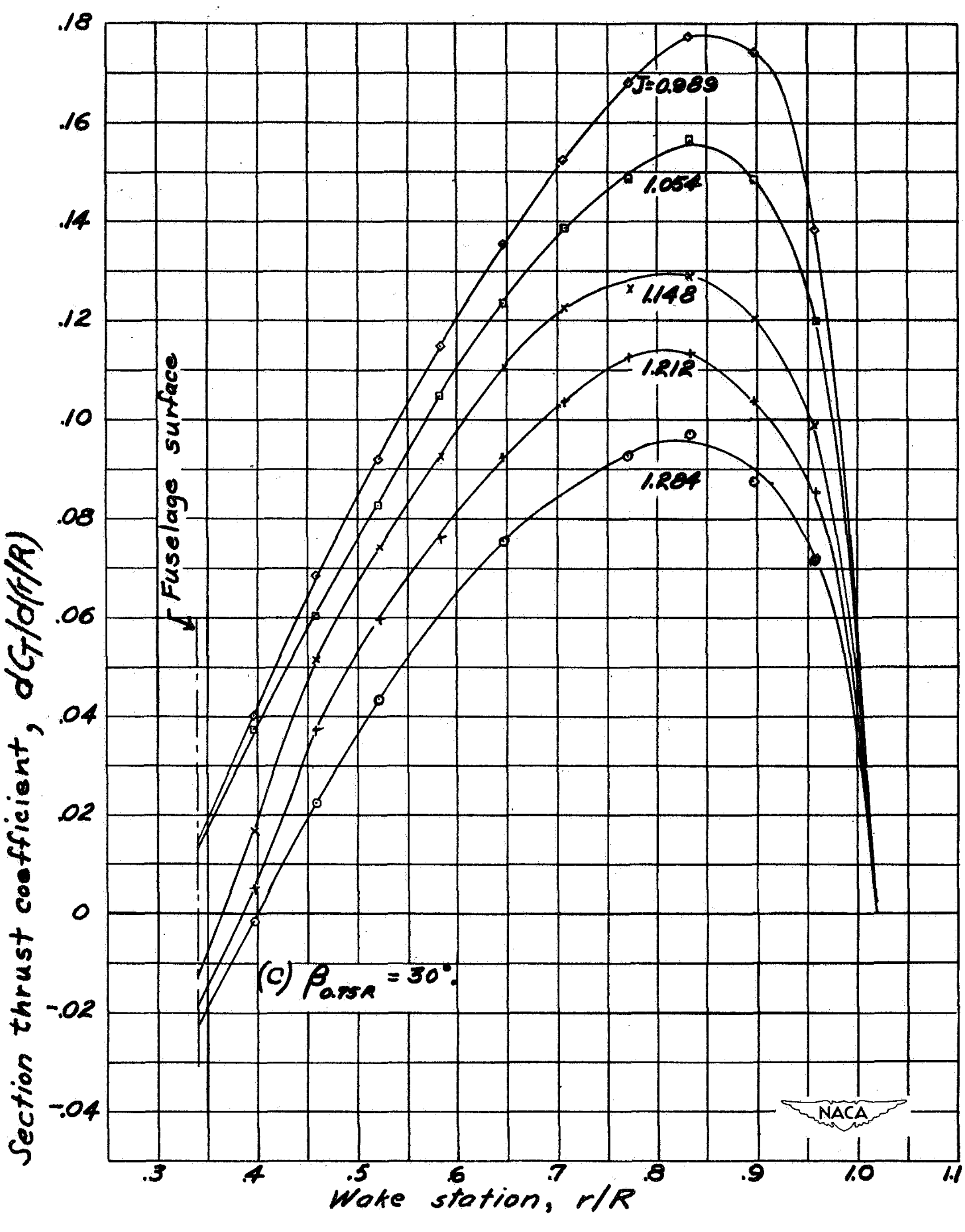

Figure 6.- Continued.

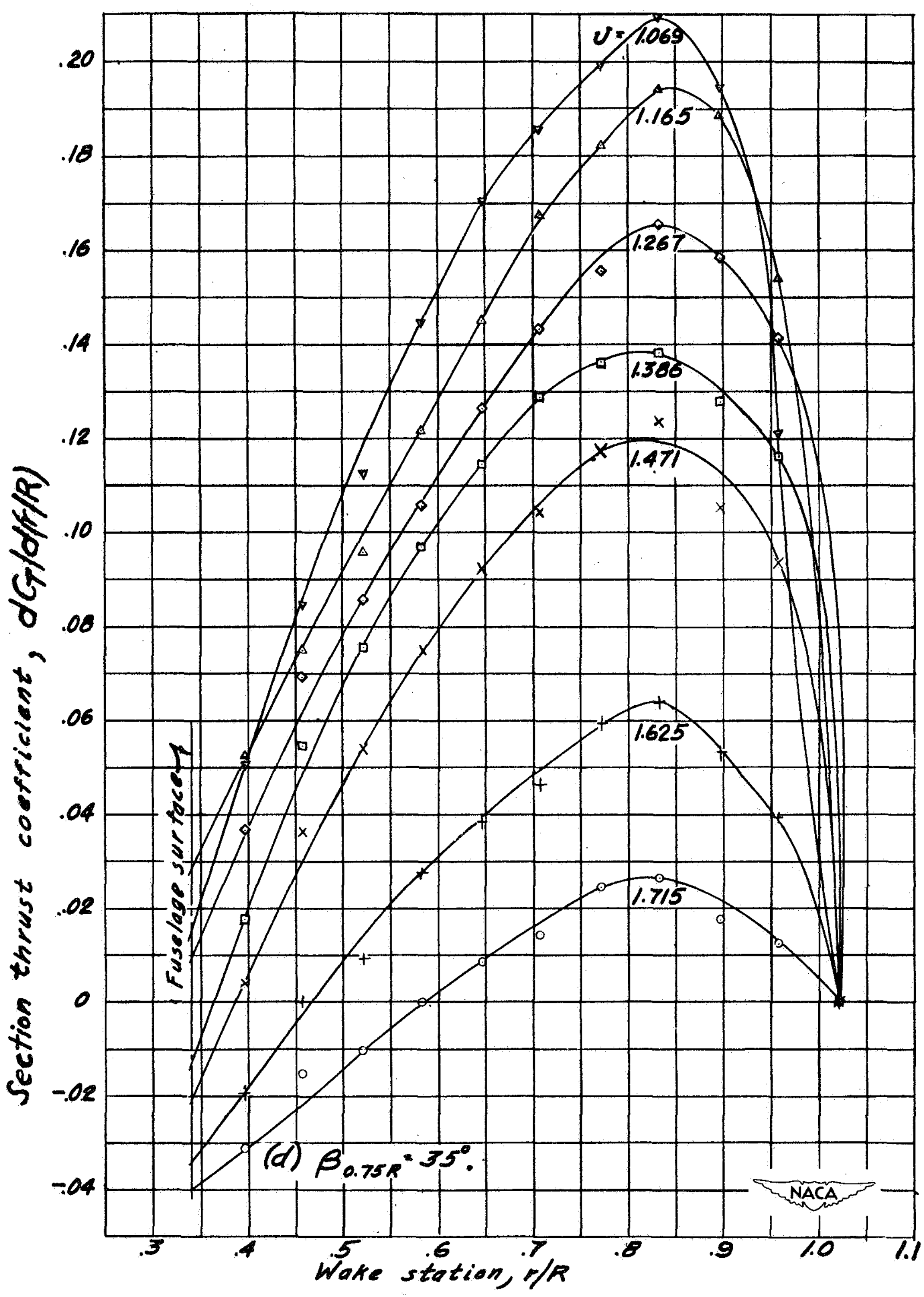

Figure 6.- Continued.

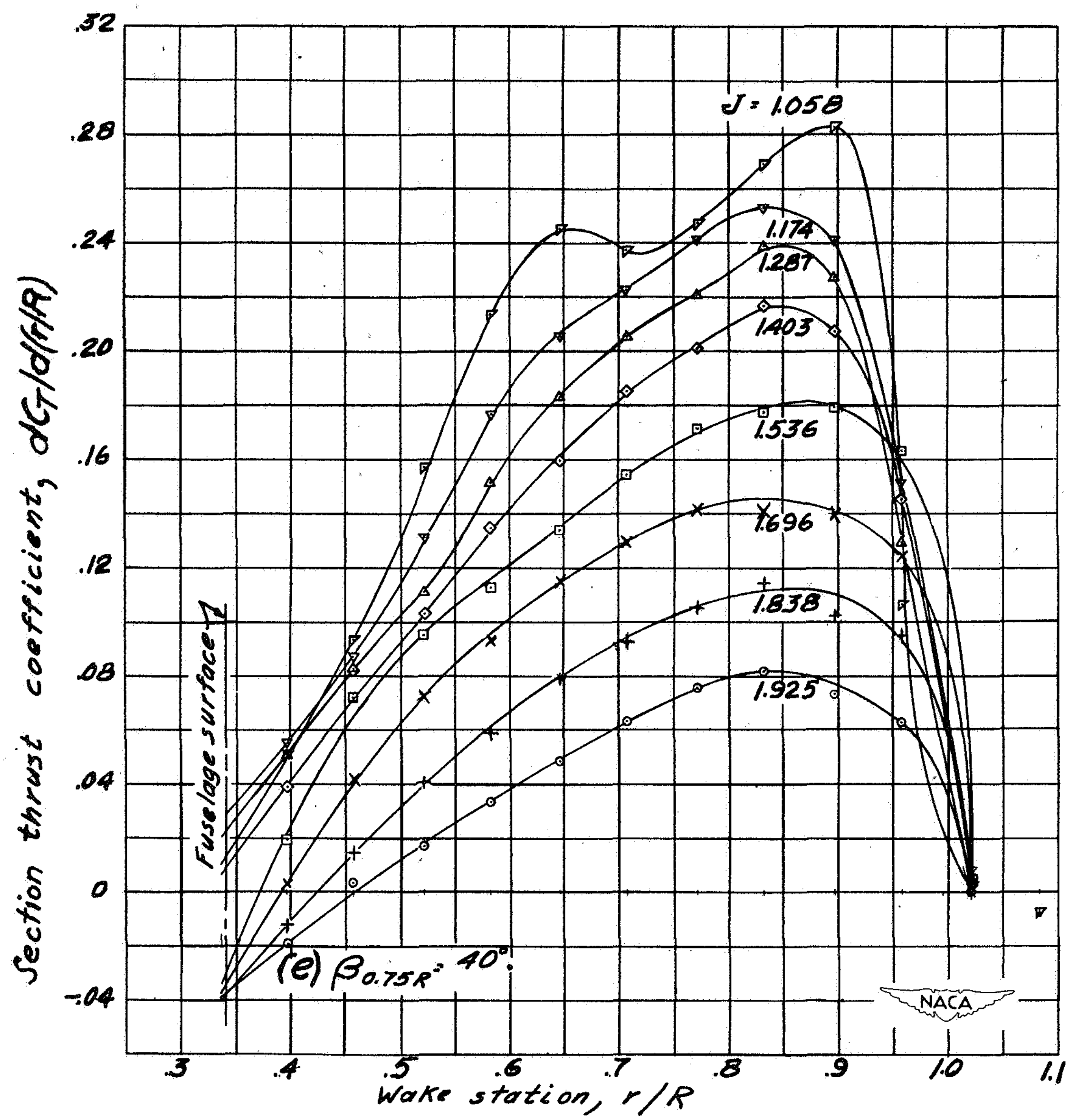

Figure 6.- Continued.

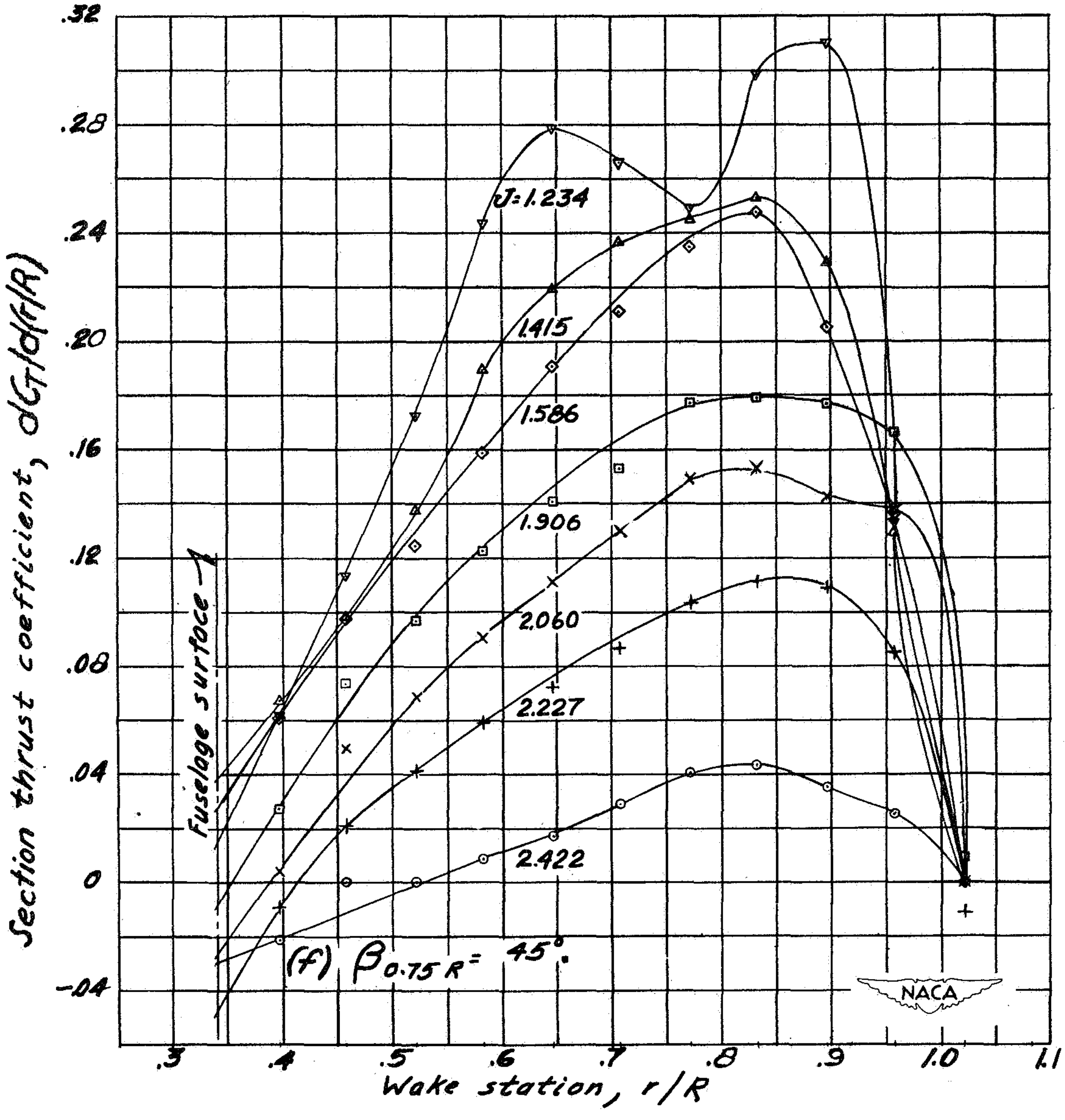

Figure 6.- Concluded.

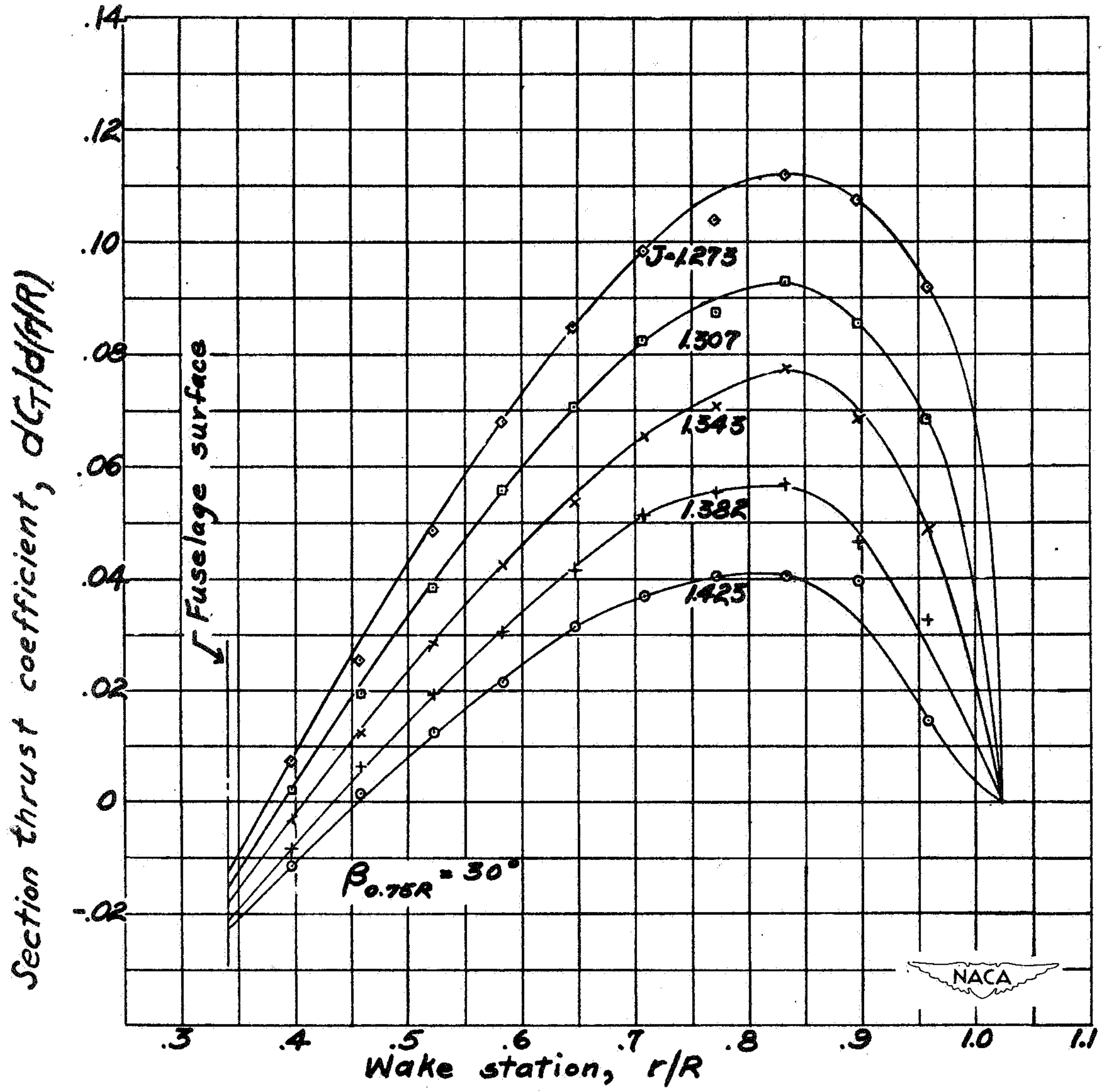

Figure 7.- Section thrust-coefficient curves for the original propeller. $M_o = 0.30$.

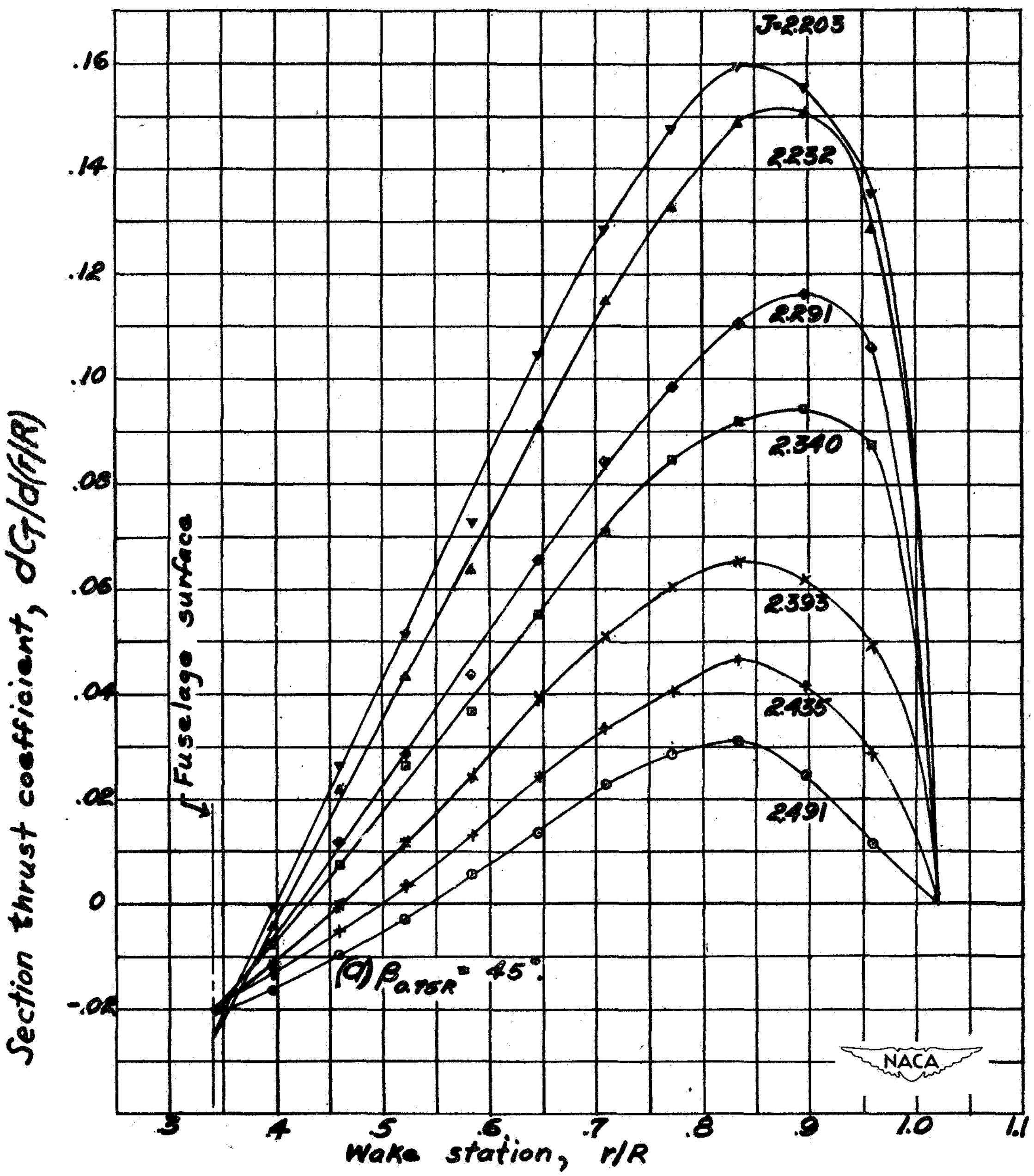

Figure 8.- Section thrust-coefficient curves for the original propeller. $M_o = 0.53$.

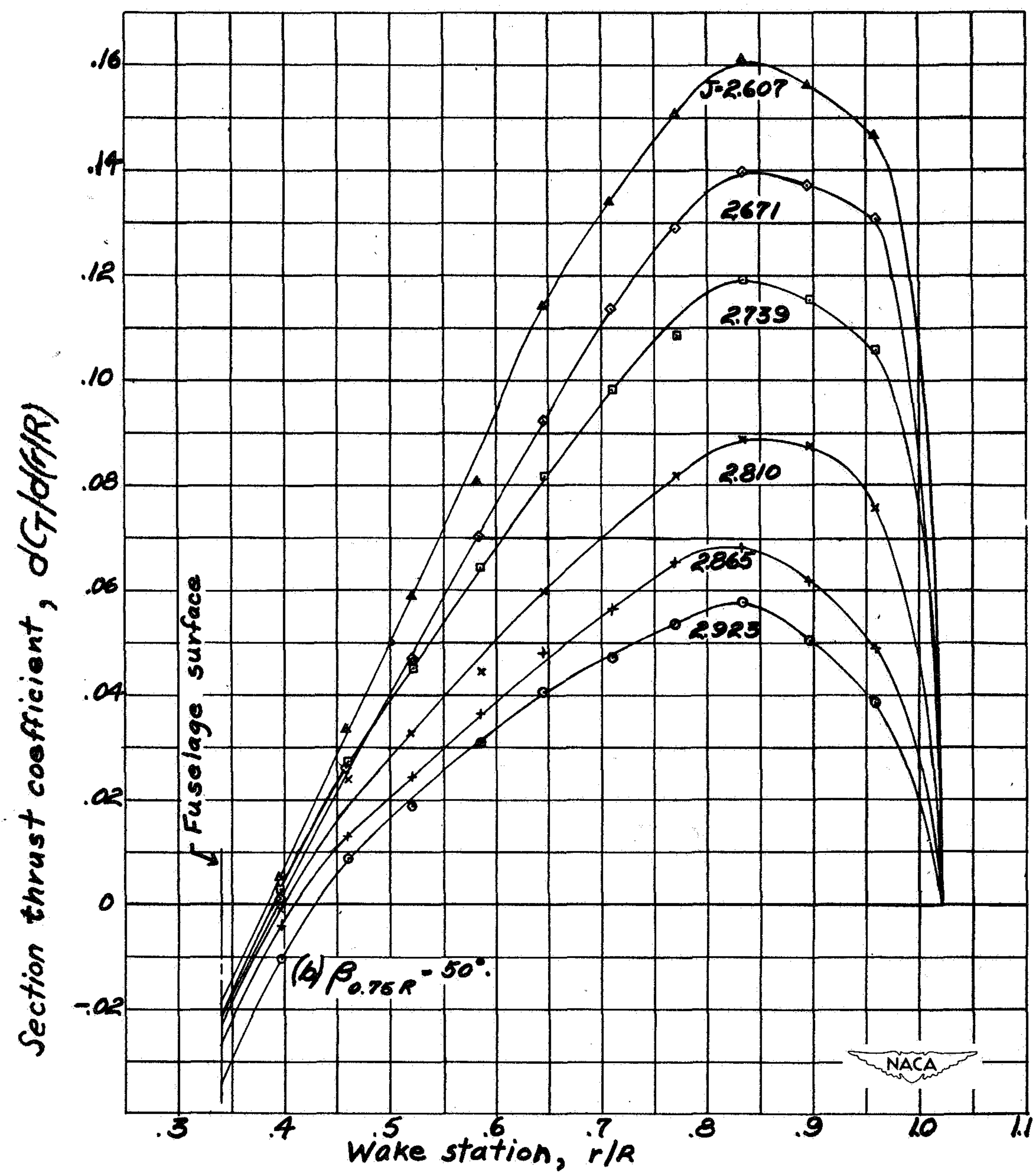

Figure 8.- Continued.

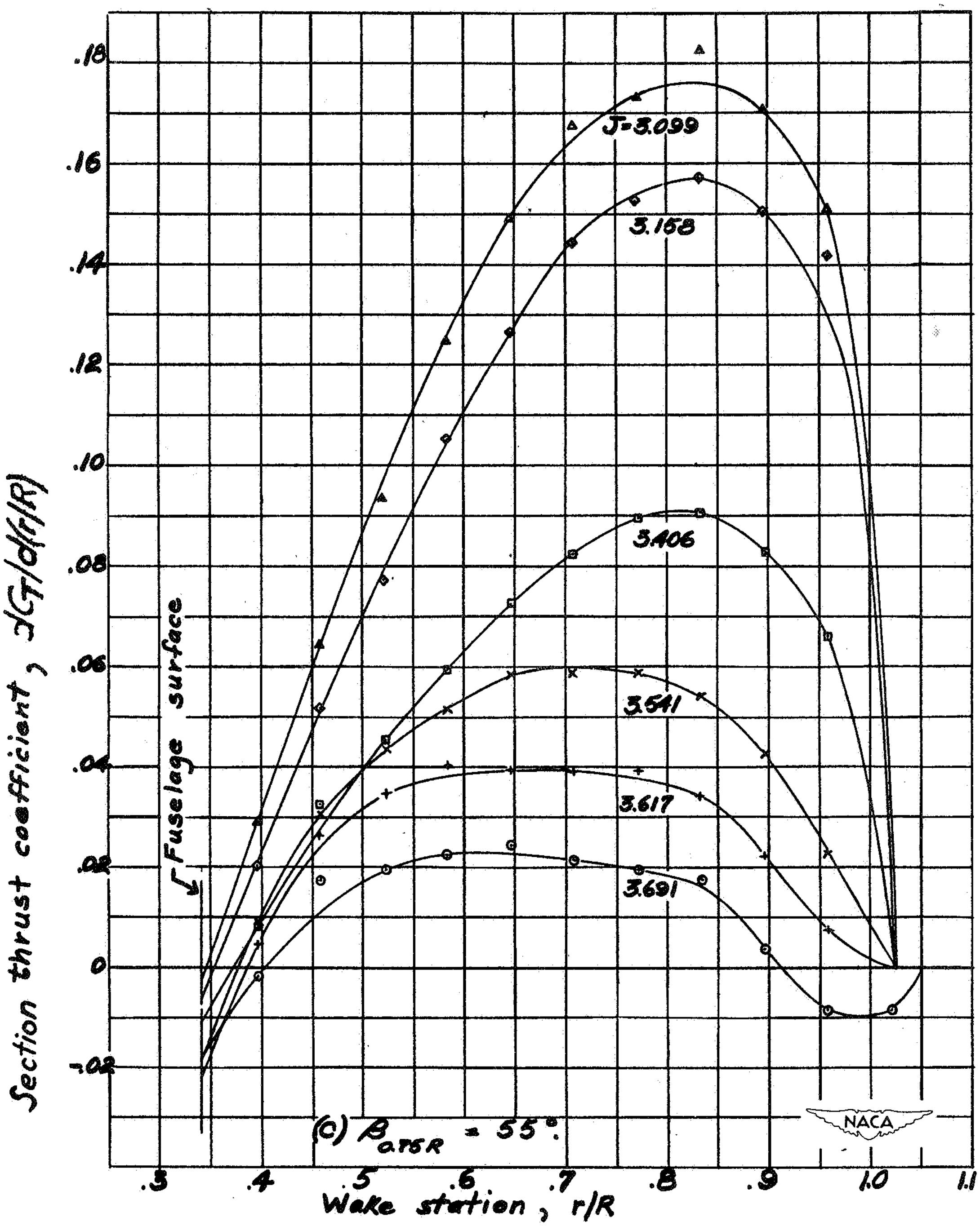

Figure 8.- Concluded.

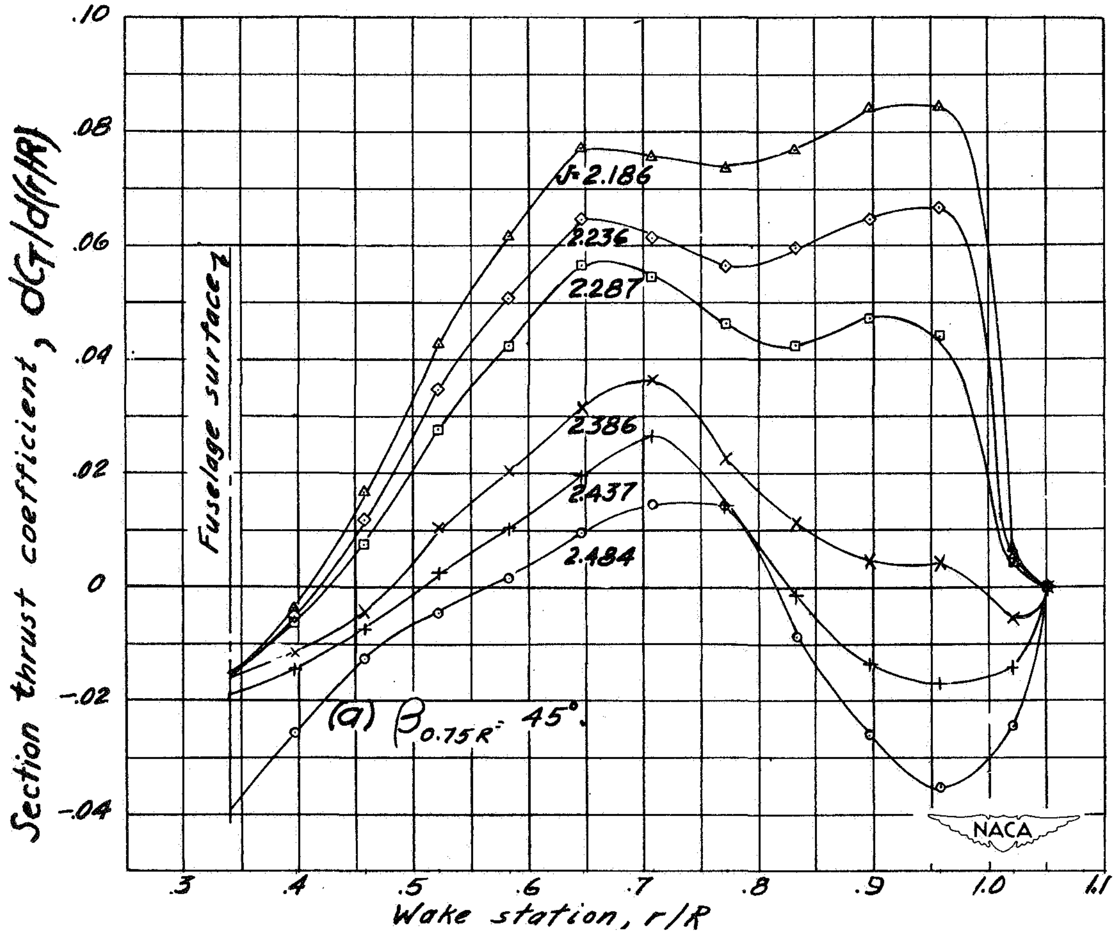

Figure 9.- Section thrust-coefficient curves for the original propeller. $M_o = 0.62$.

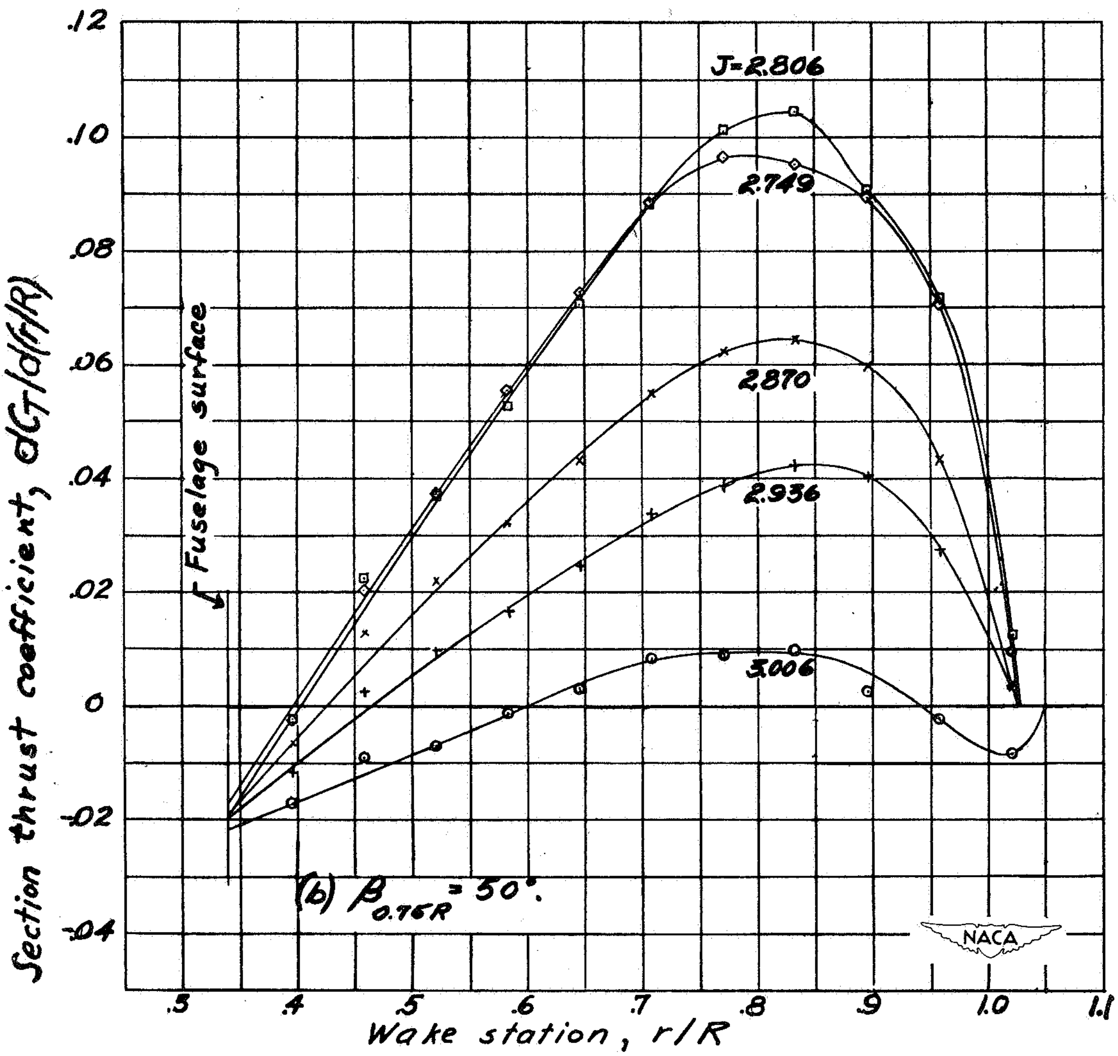

Figure 9.- Continued.

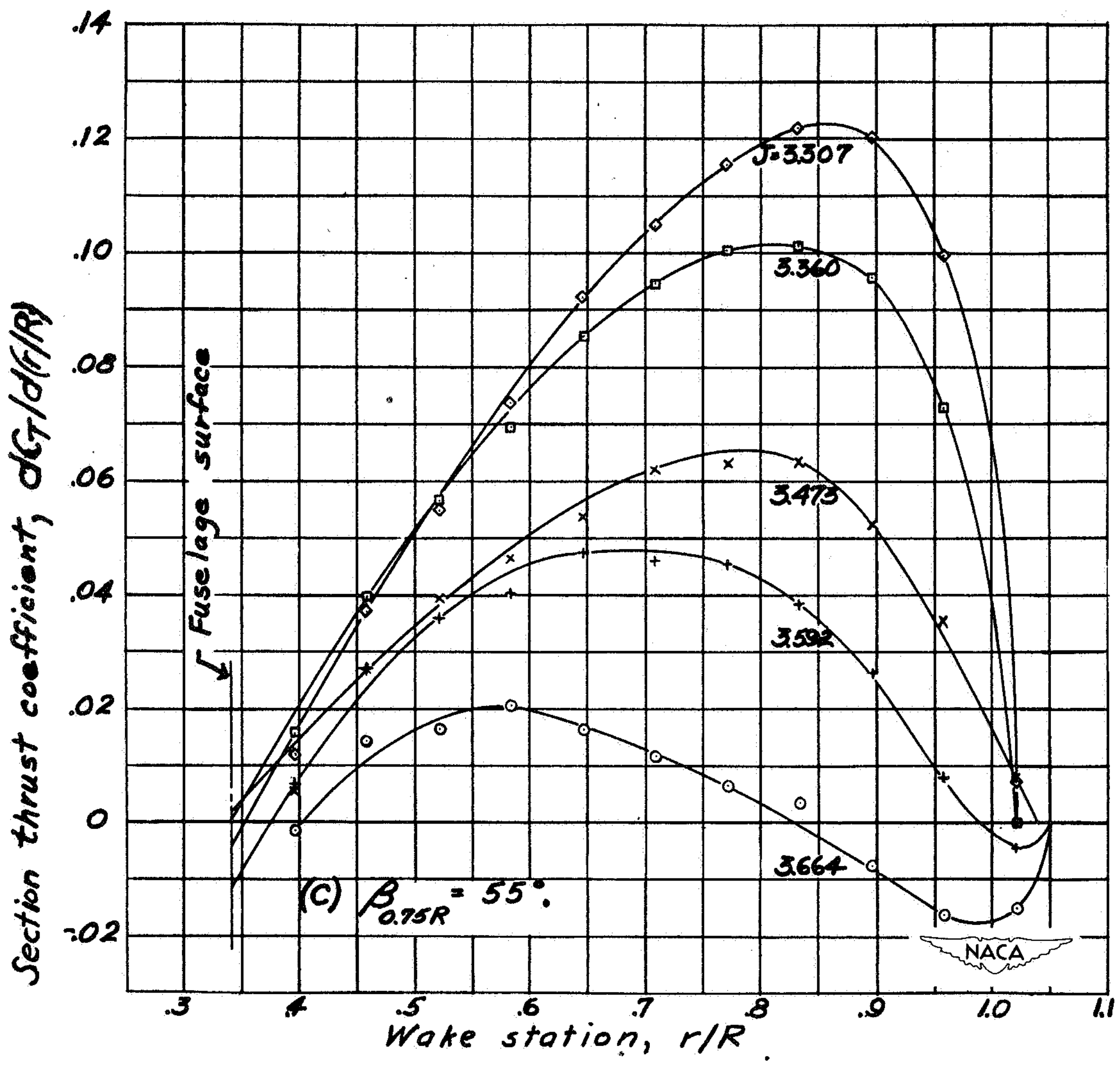

Figure 9.- Concluded.

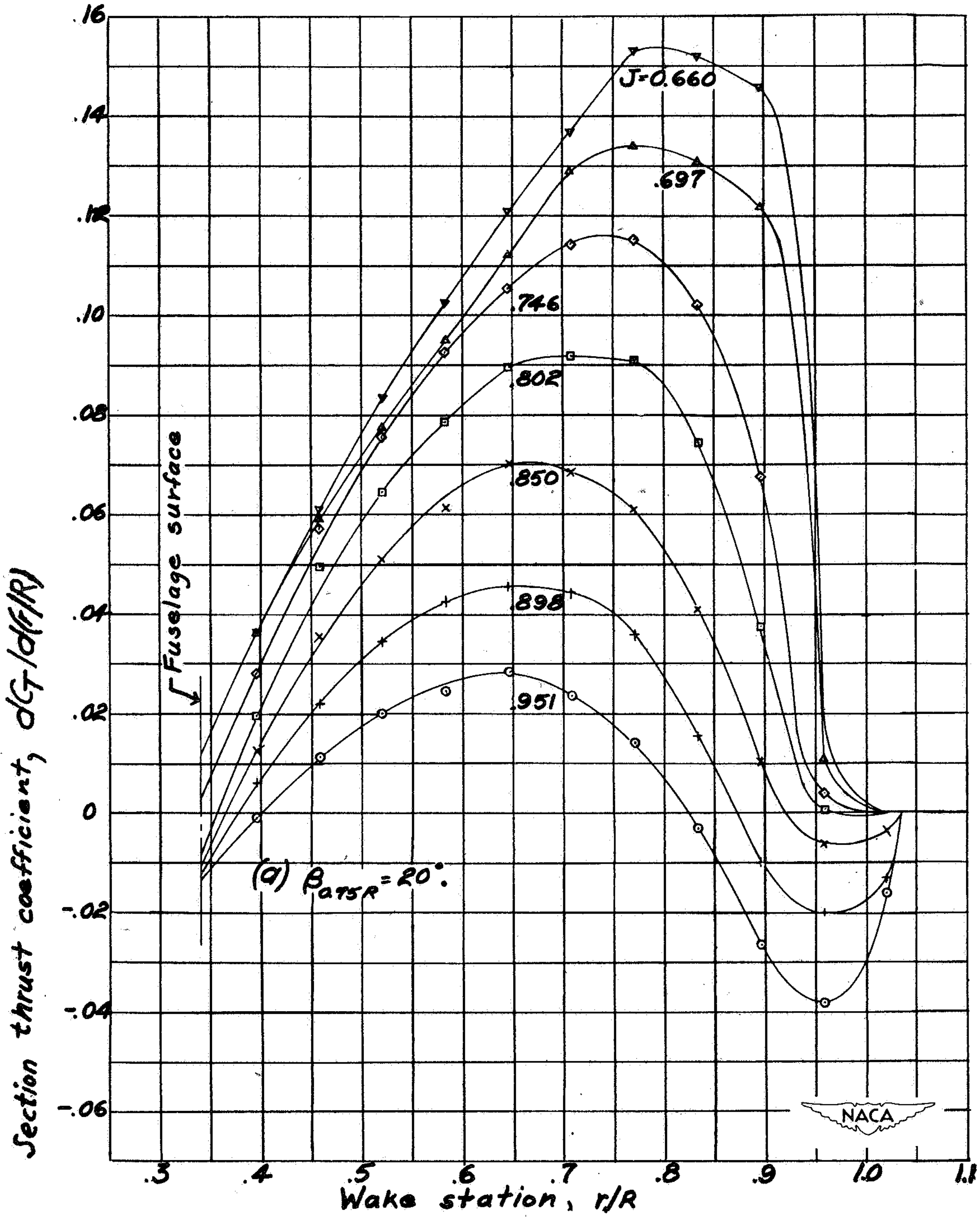

Figure 10.- Section thrust-coefficient curves for the modified propeller. $M_o = 0.20$.

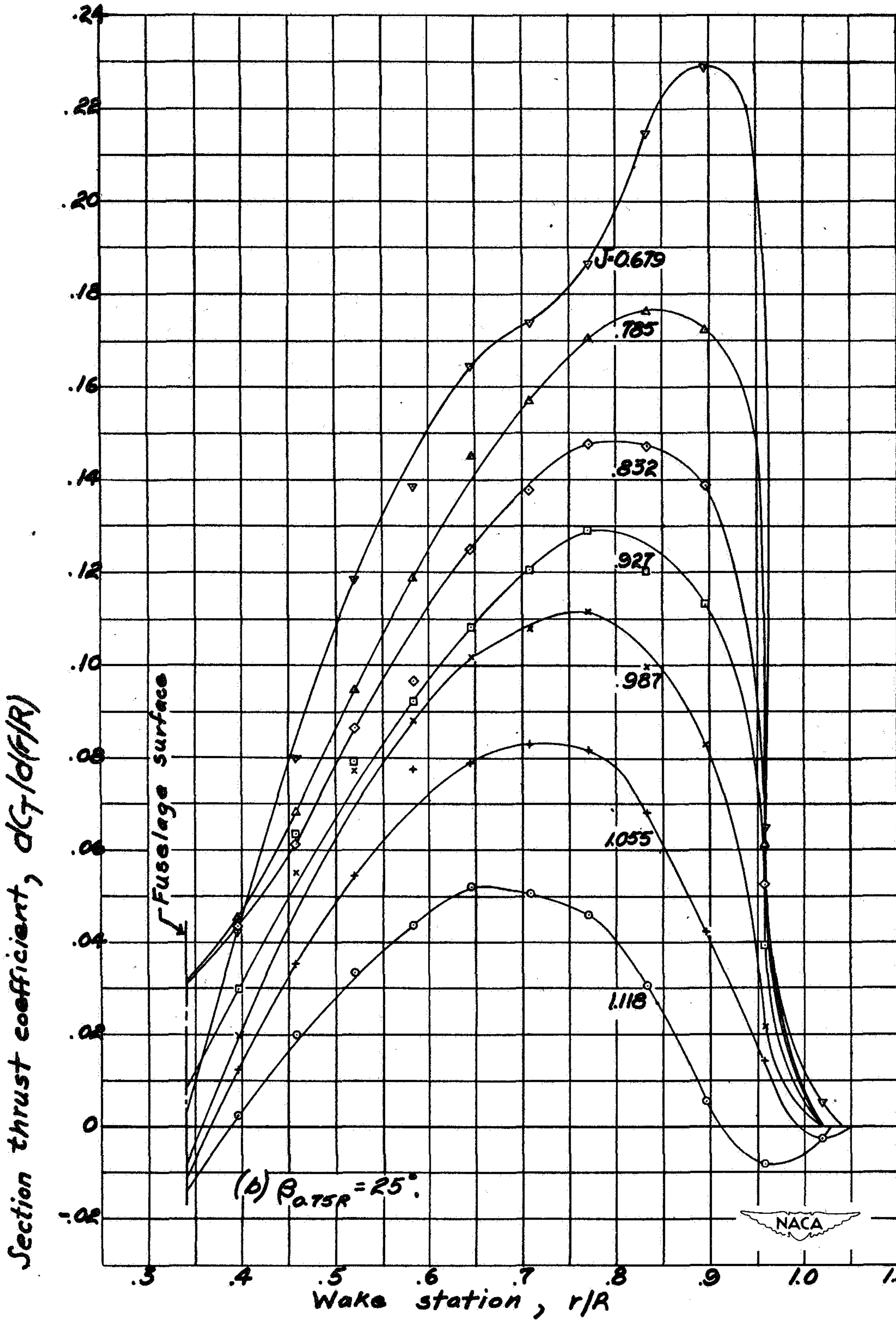

Figure 10.- Continued.

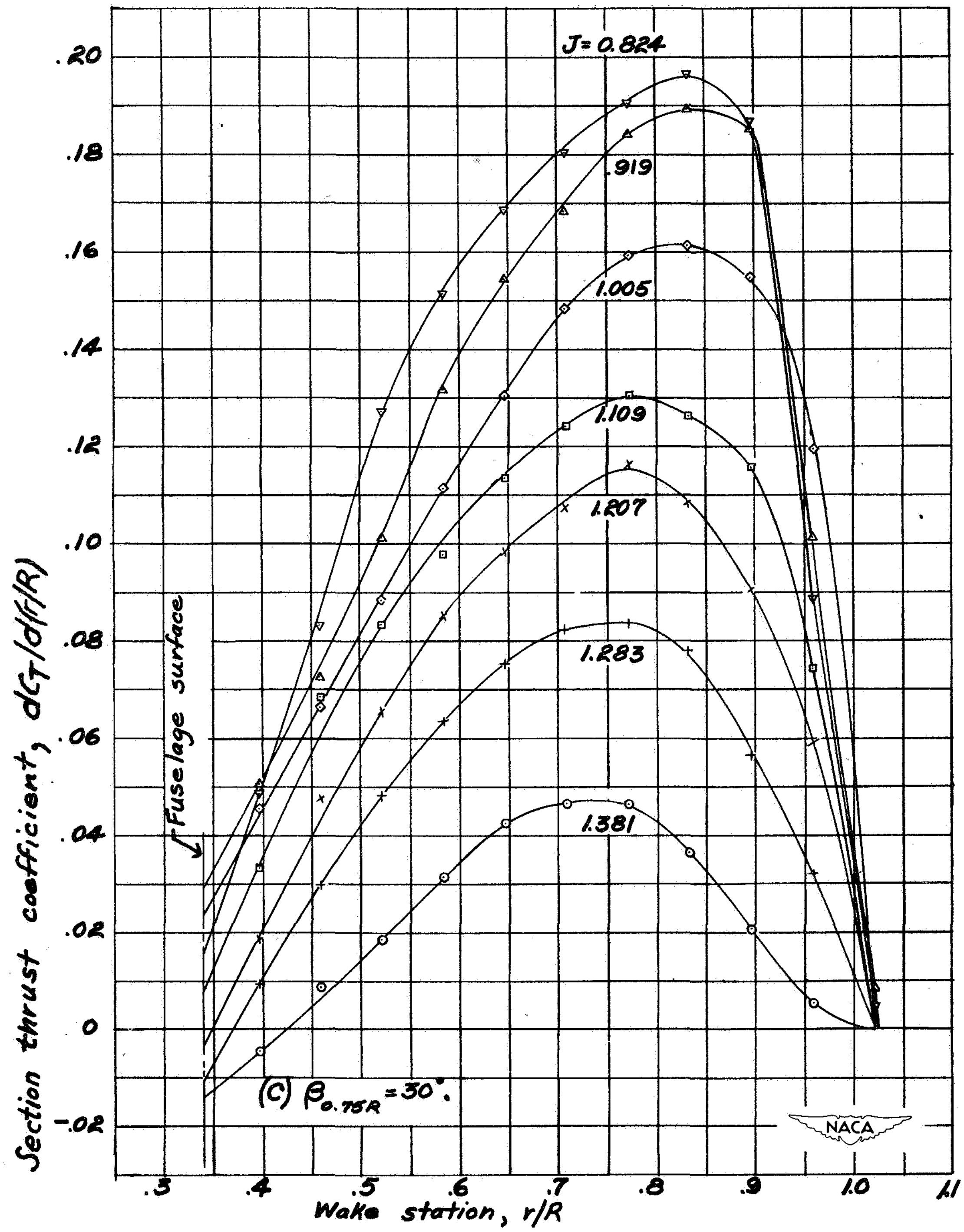

Figure 10.- Continued.

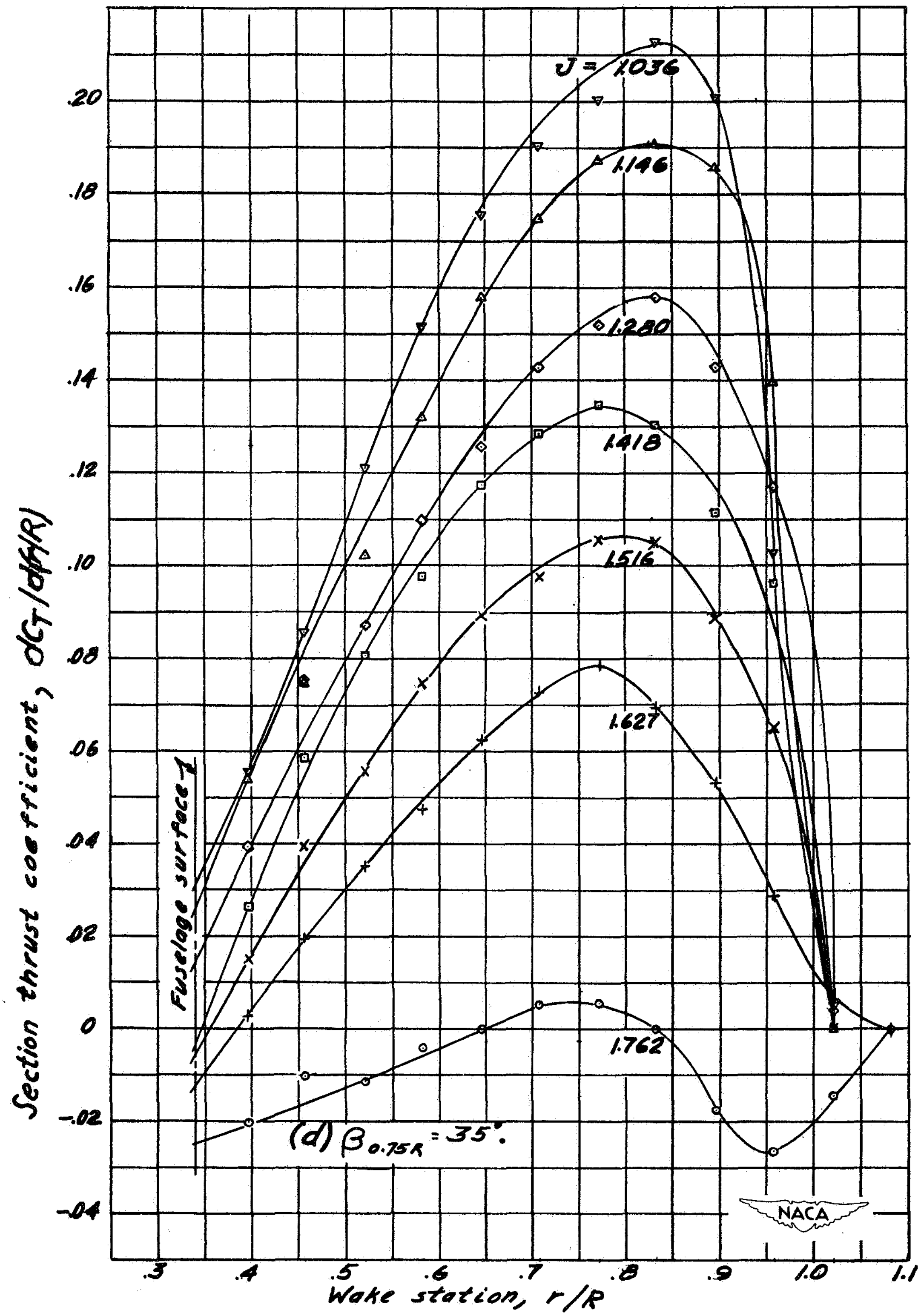

Figure 10.- Continued.

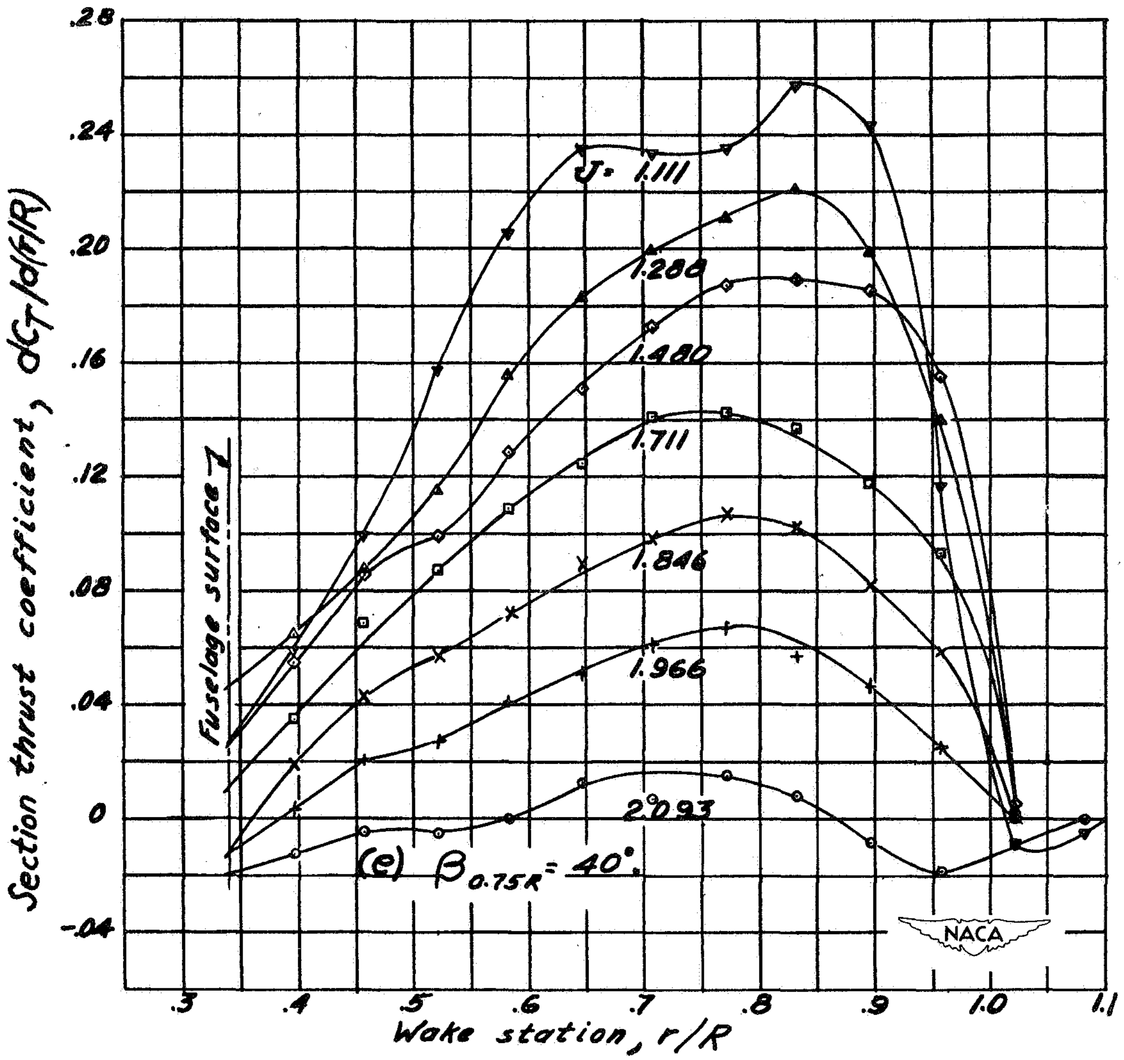

Figure 10.- Continued.

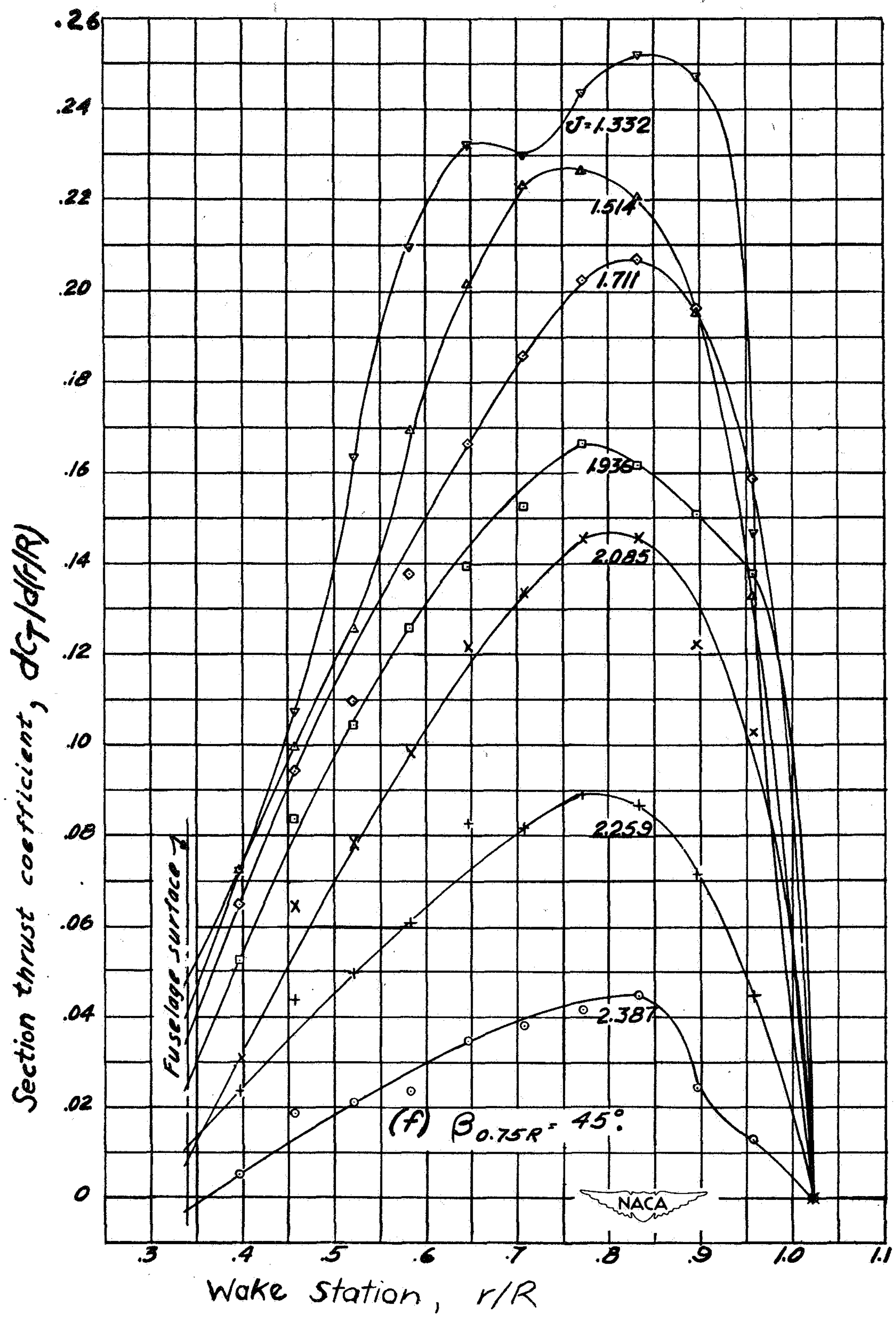

Figure 10.- Concluded.

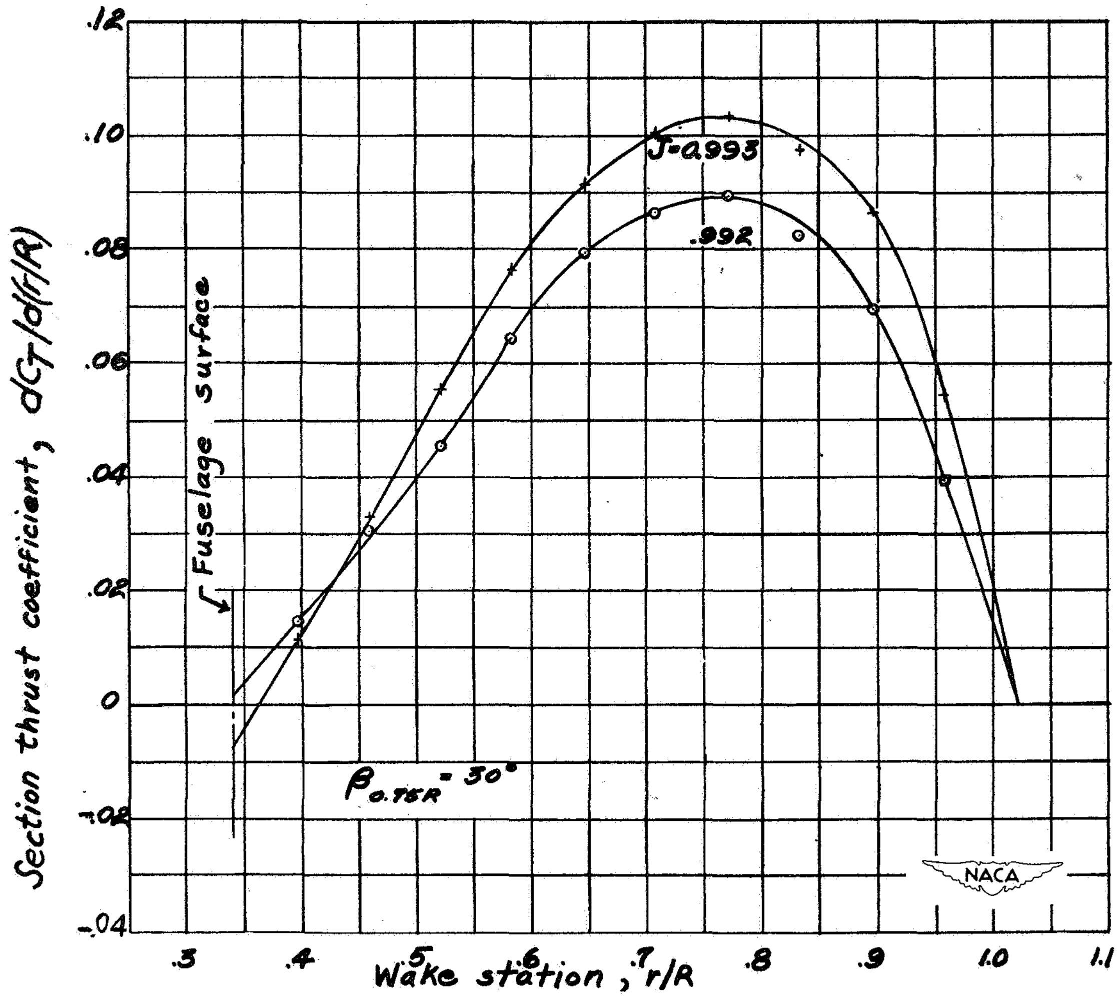

Figure 11.- Section thrust-coefficient curves for the modified propeller. $M_o = 0.30$.

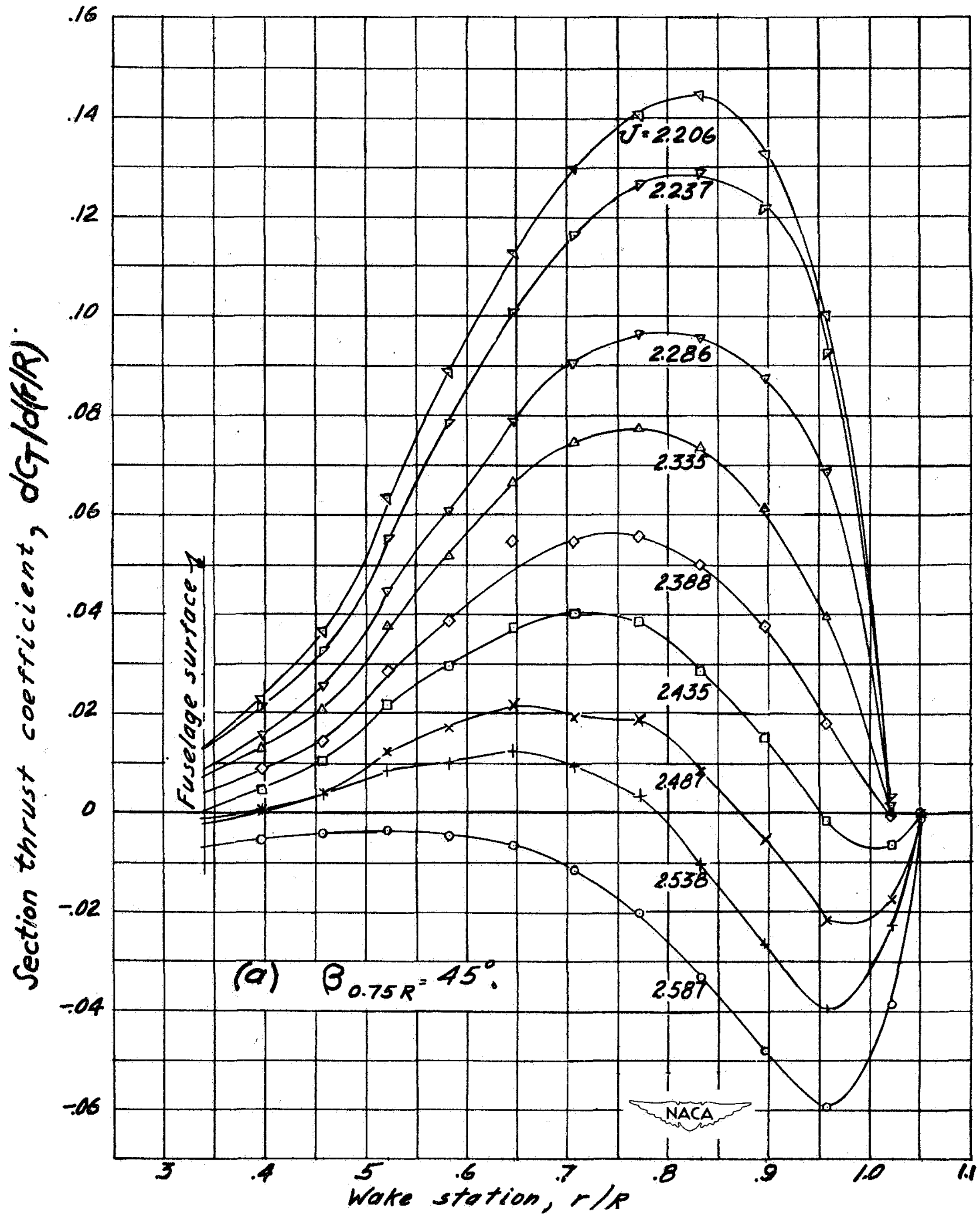

Figure 12.- Section thrust-coefficient curves for the modified propeller. $M_o = 0.53$.

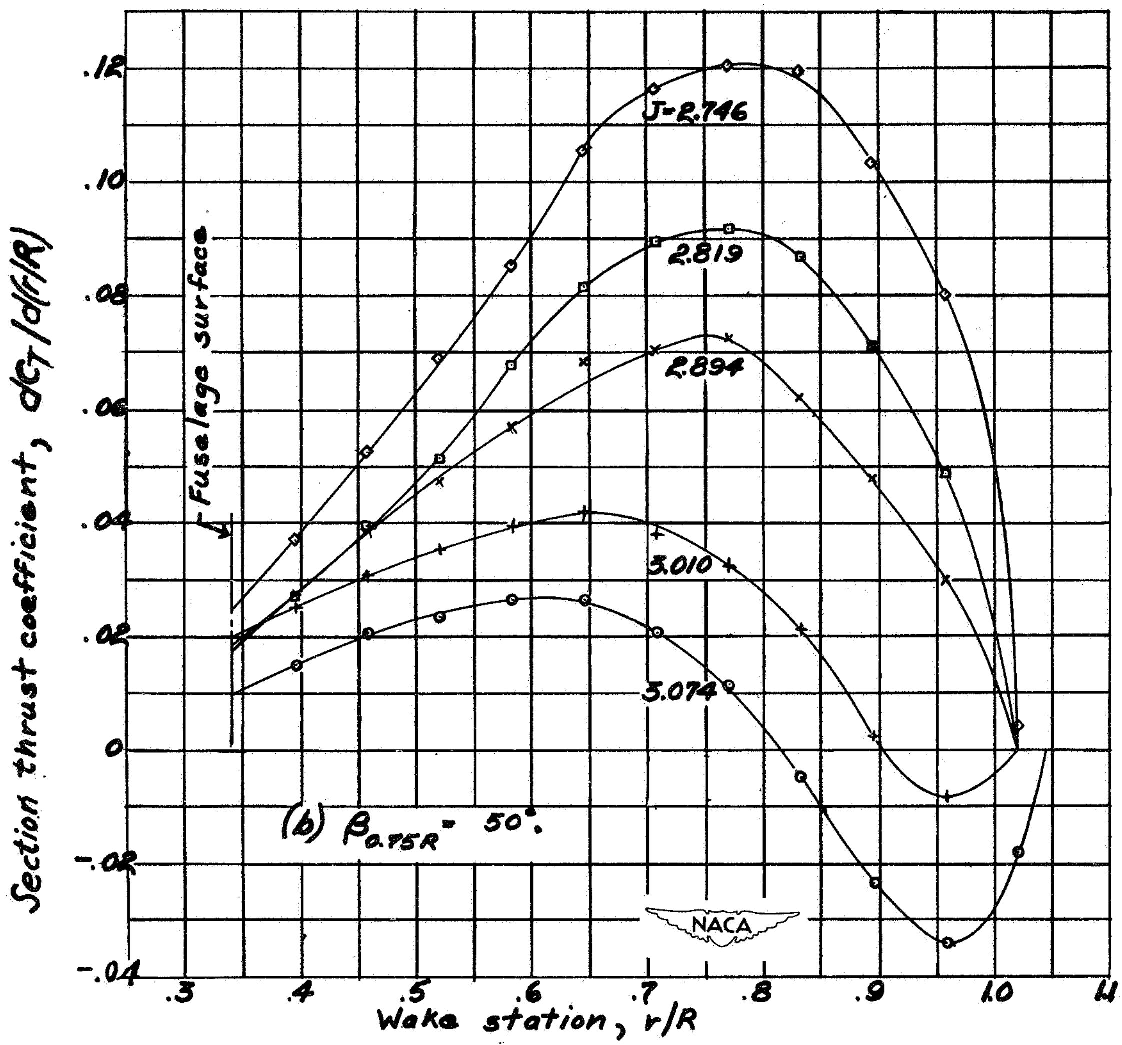

Figure 12.- Continued.

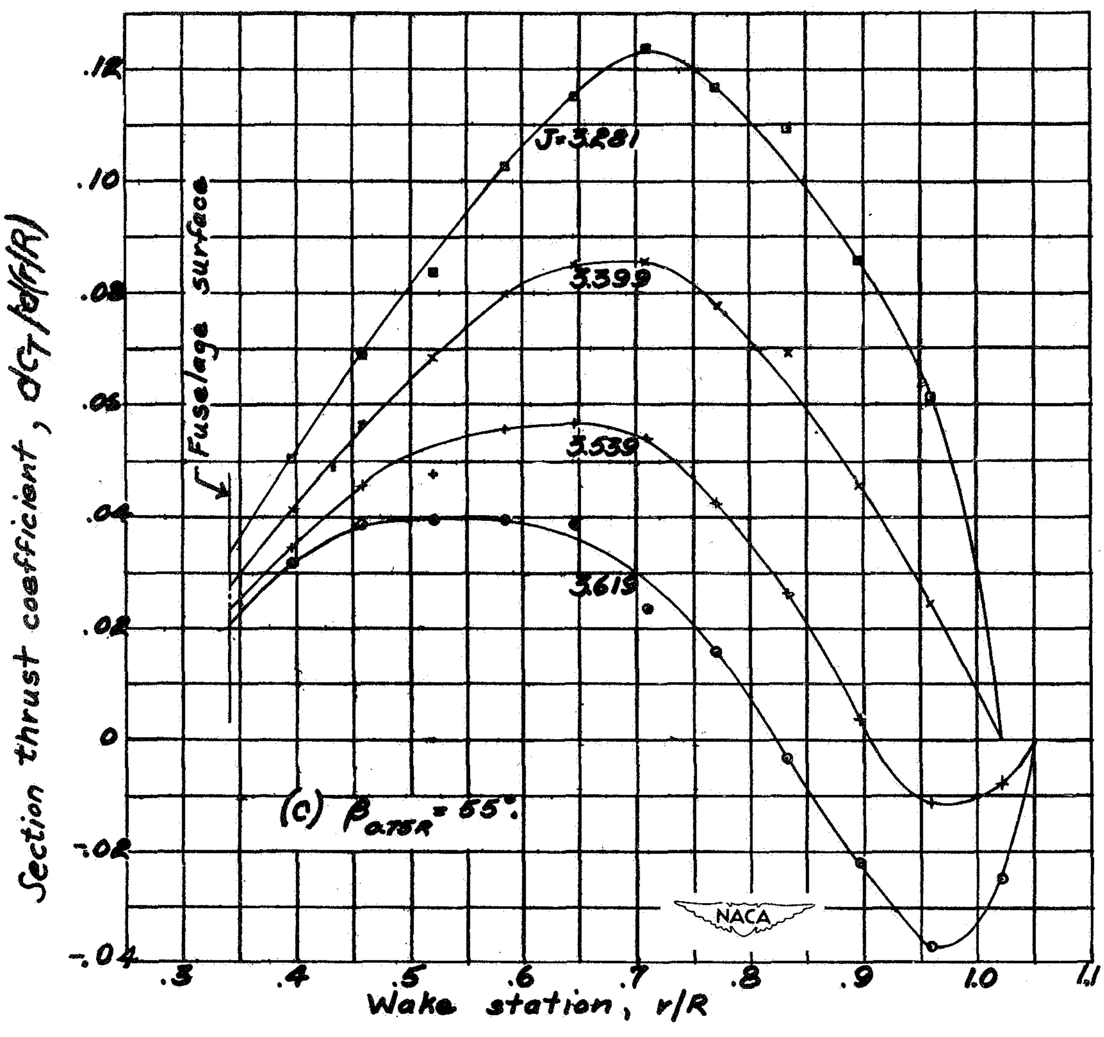

Figure 12.- Concluded.

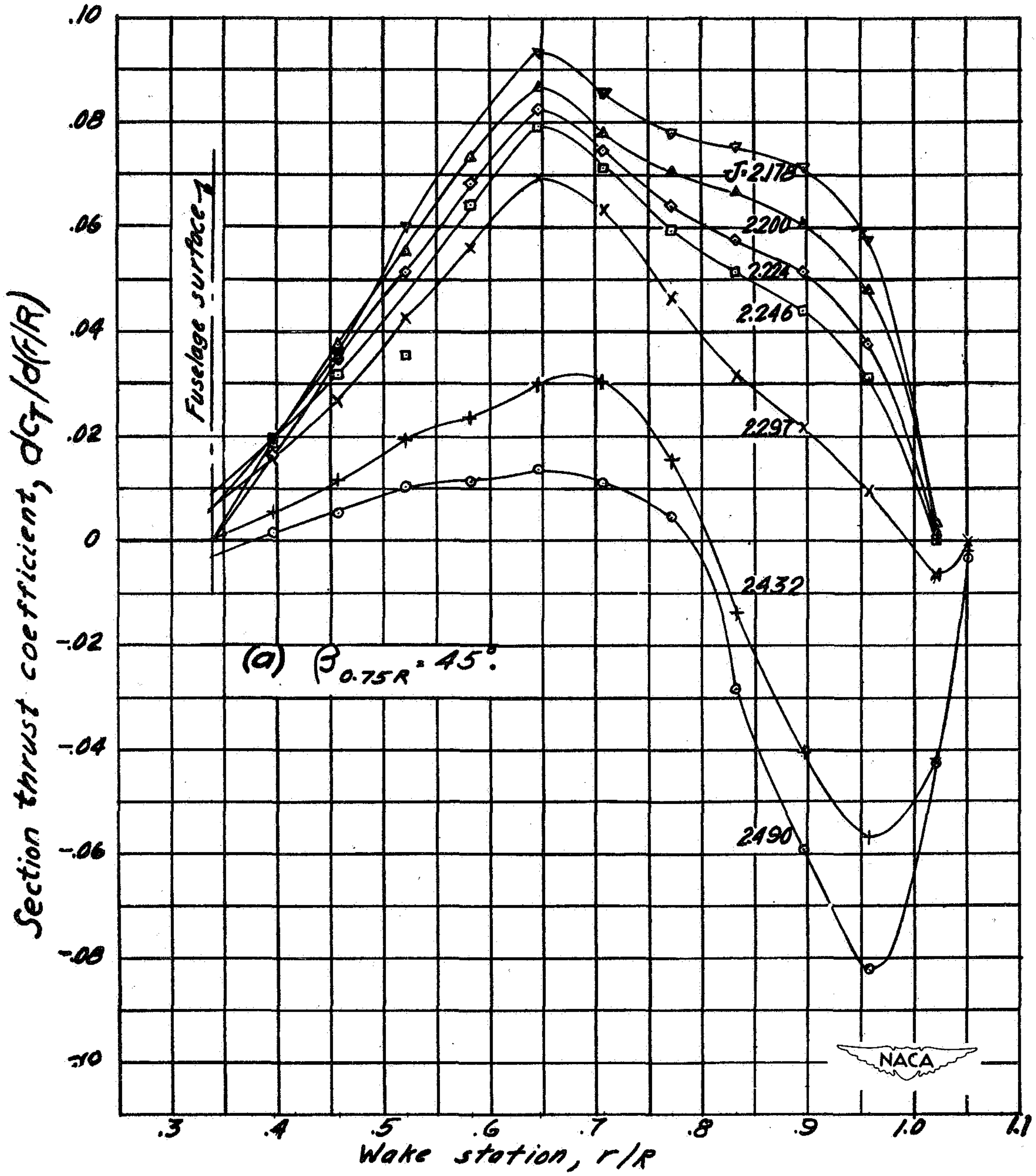

Figure 13.- Section thrust-coefficient curves for the modified propeller. $M_o = 0.62$.

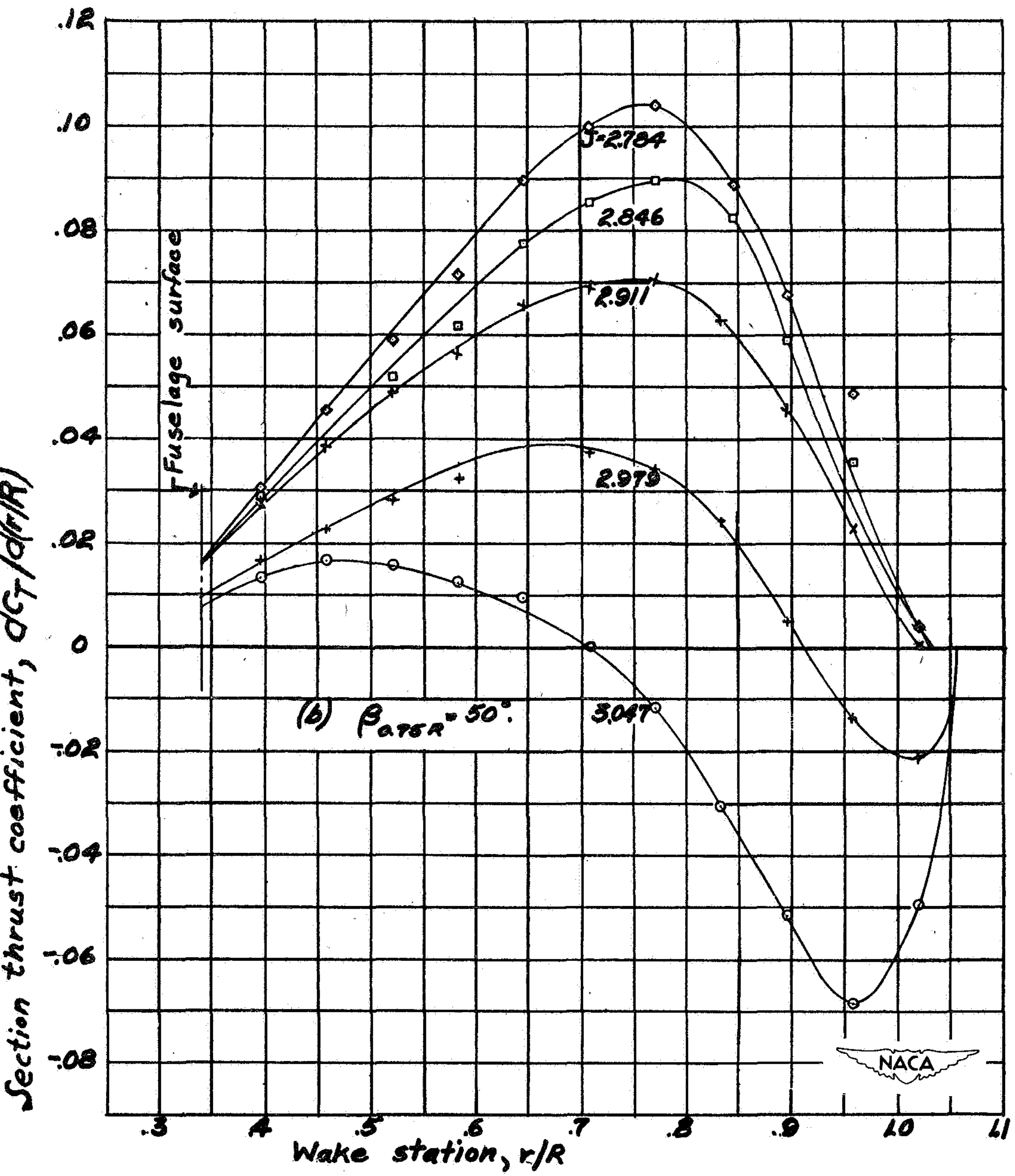

Figure 13.- Continued.

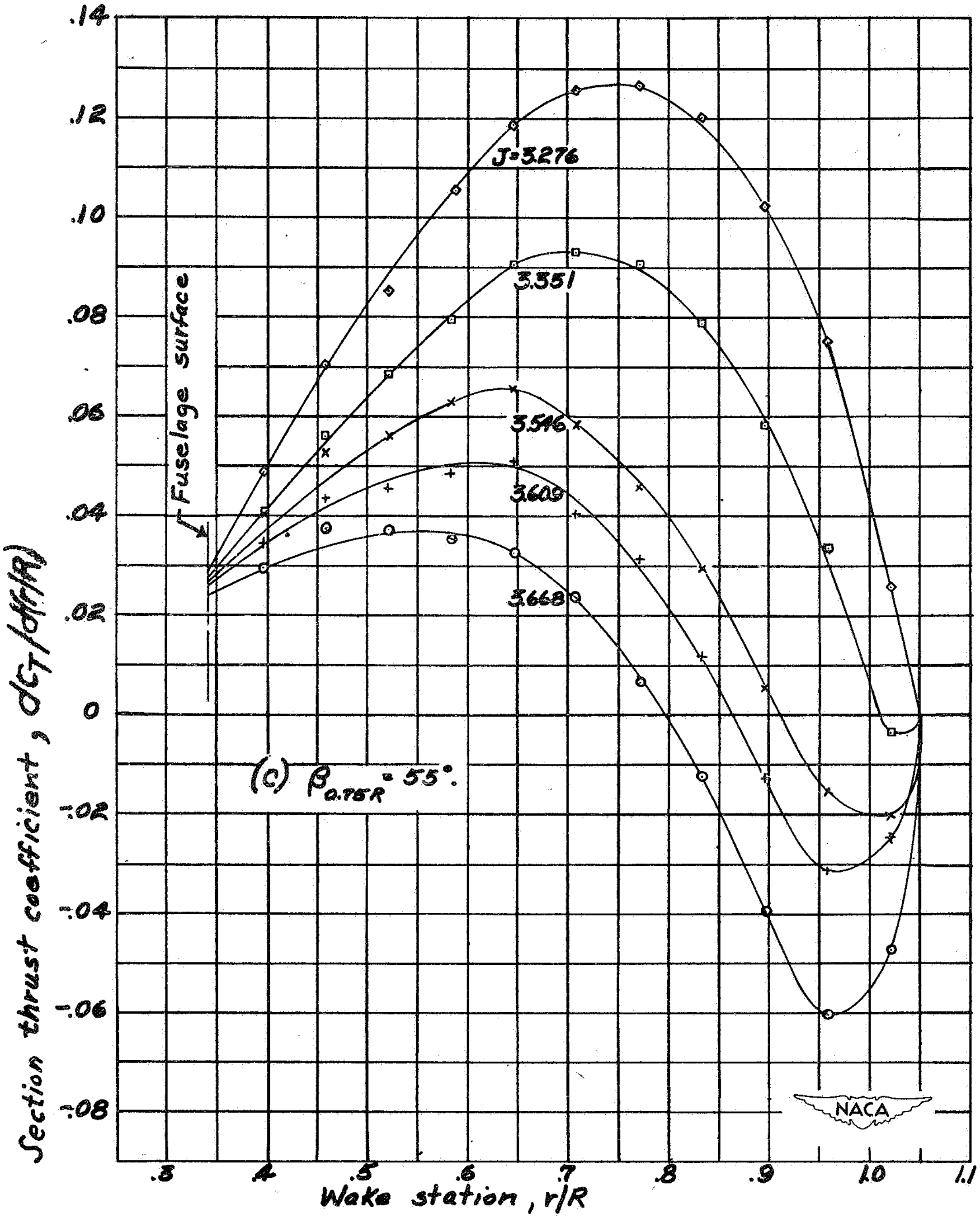

Figure 13.- Concluded.

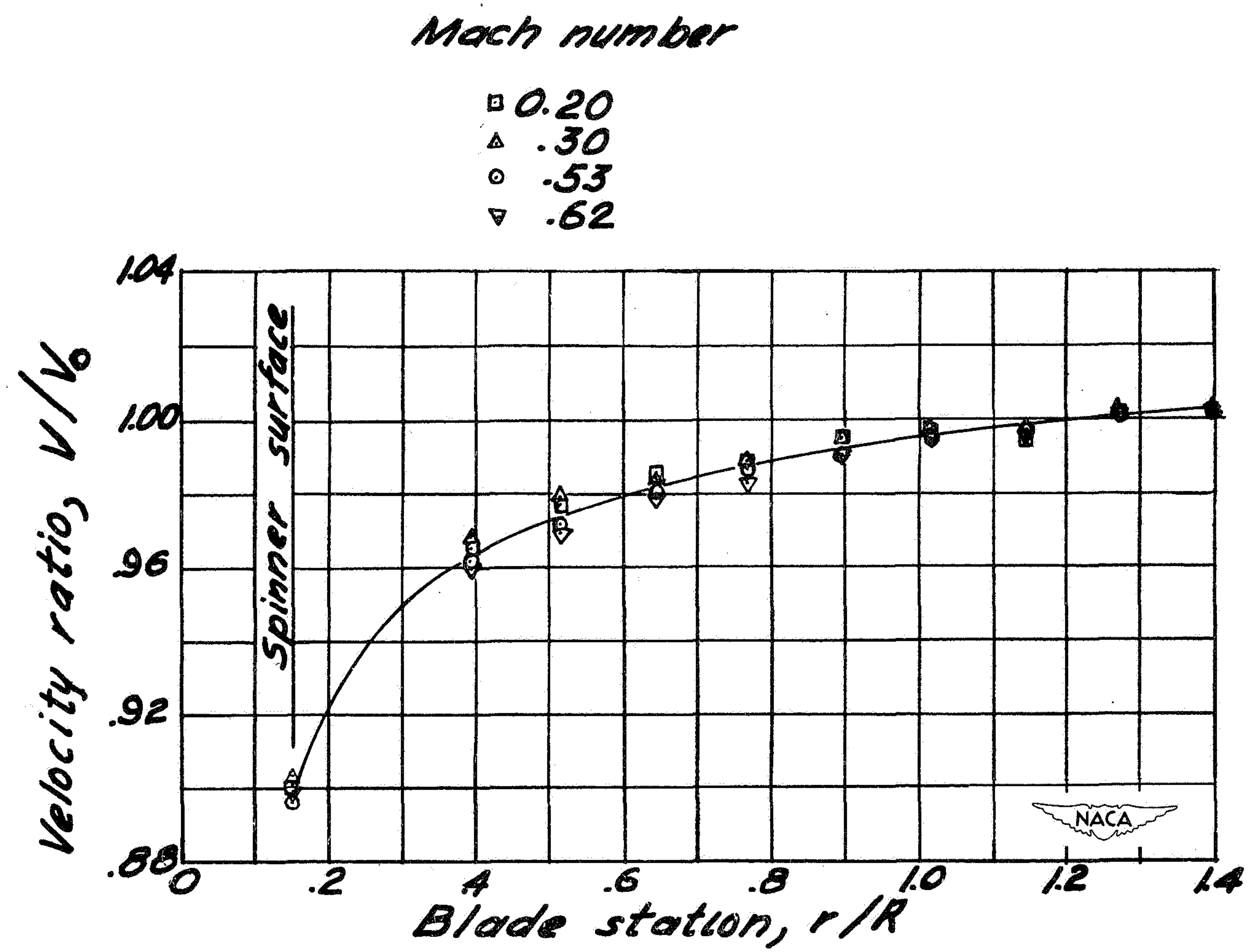

Figure 14.- Velocity survey at plane of propeller for basic model without propeller.

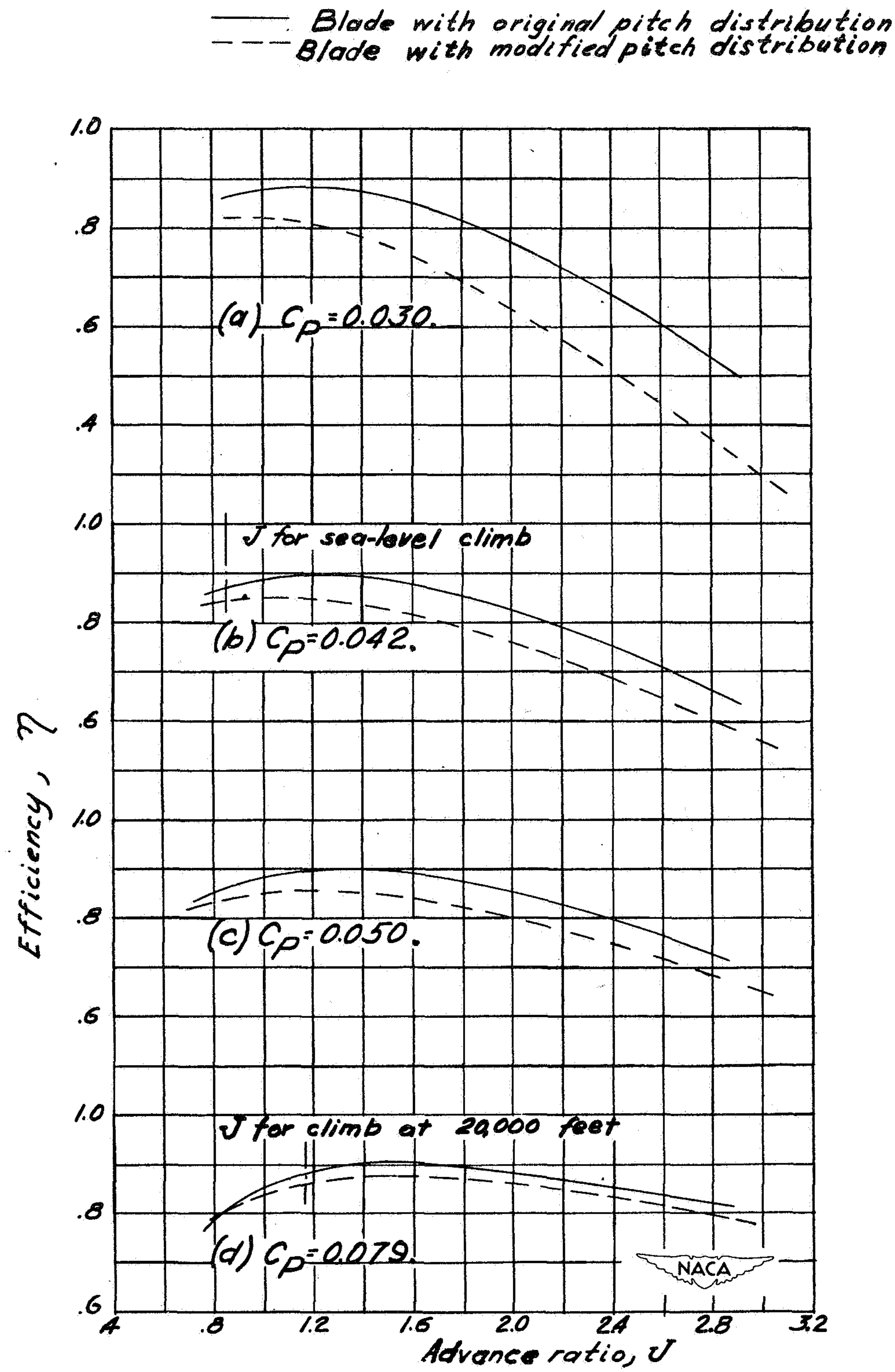

Figure 15.- Effect on efficiency of operation at constant power coefficient. $M_o = 0.20$.

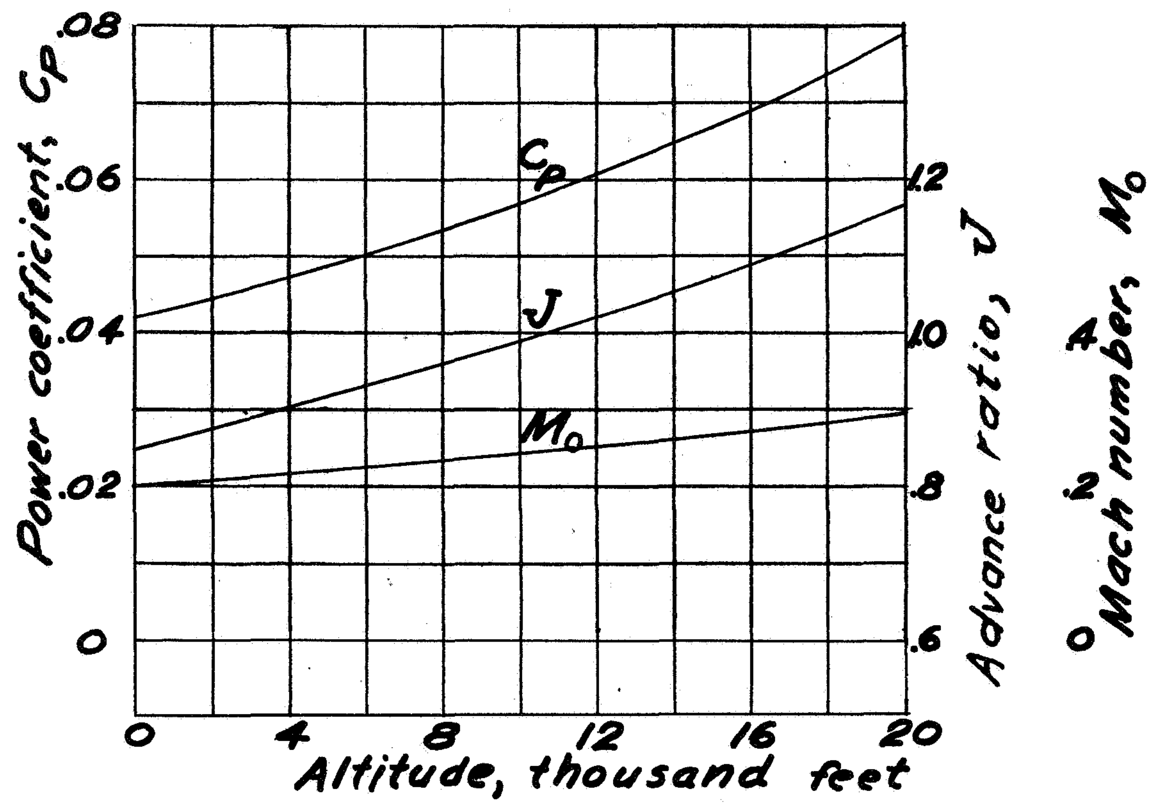

(a) Climb operating conditions.

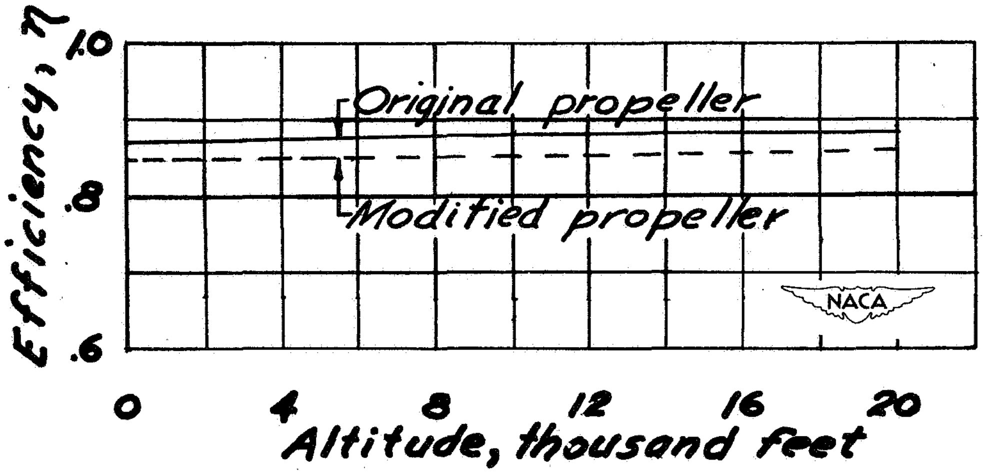

(b) Climb performance.

Figure 16.- Climb operating conditions and climb performance.

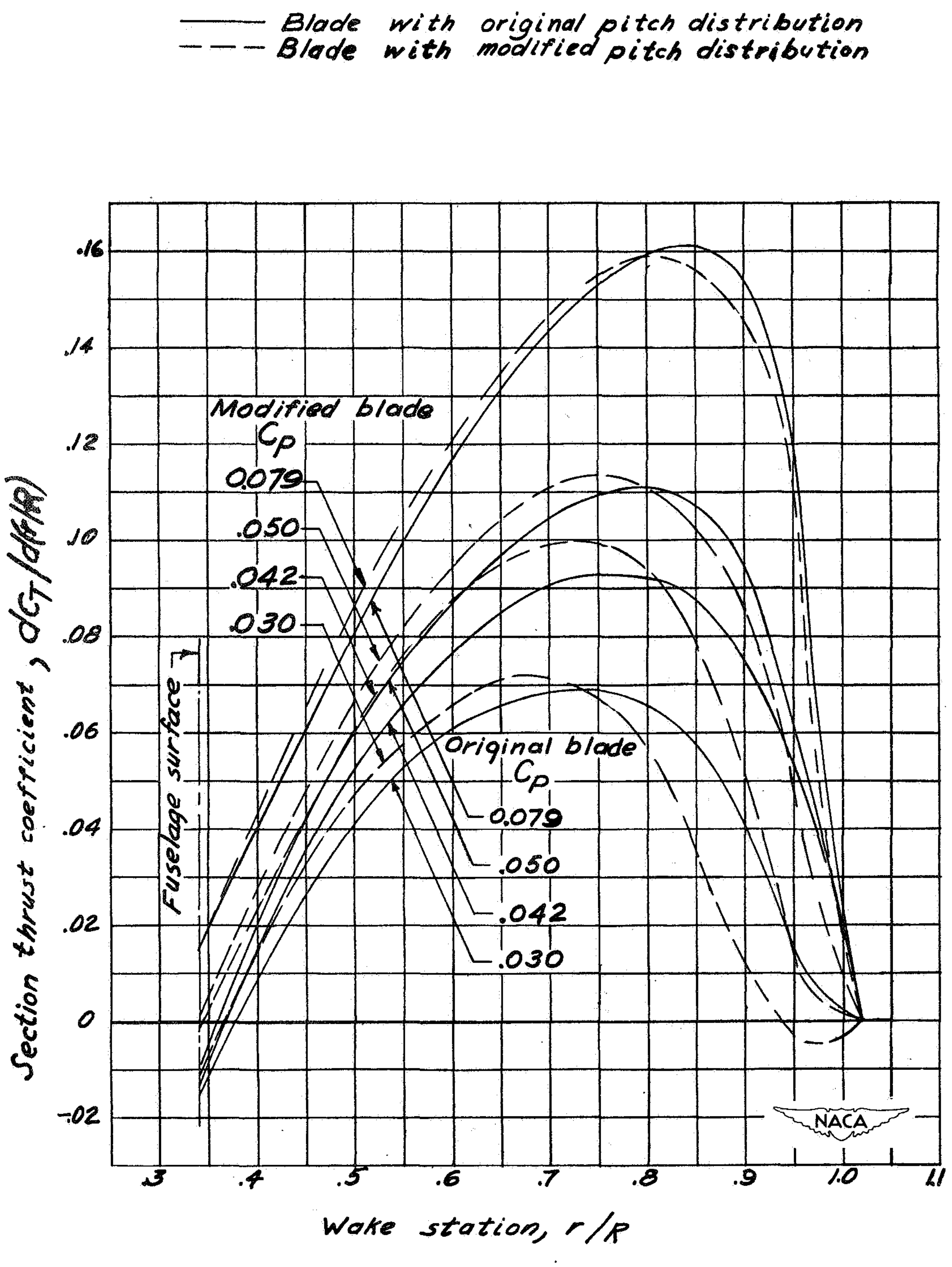

Figure 17.- Comparison of section thrust-coefficient curves at constant power coefficients for the climb condition. $M_0 = 0.20$; $J = 0.85$.

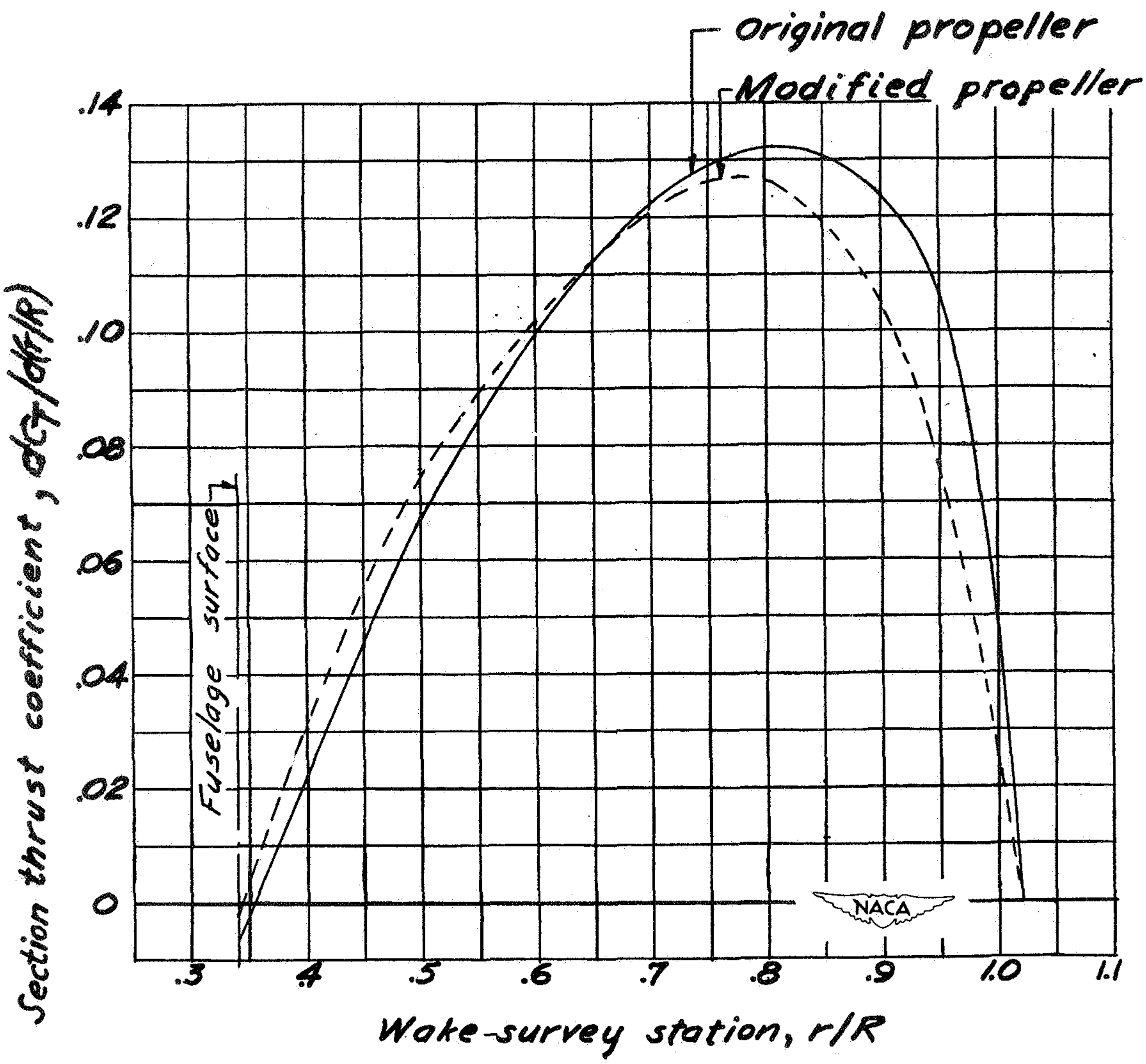

Figure 18.- Comparison of section thrust-coefficient curves for the climb condition at an altitude of 20,000 feet. $M_0 = 0.20$; $J = 1.165$; $C_P = 0.079$.

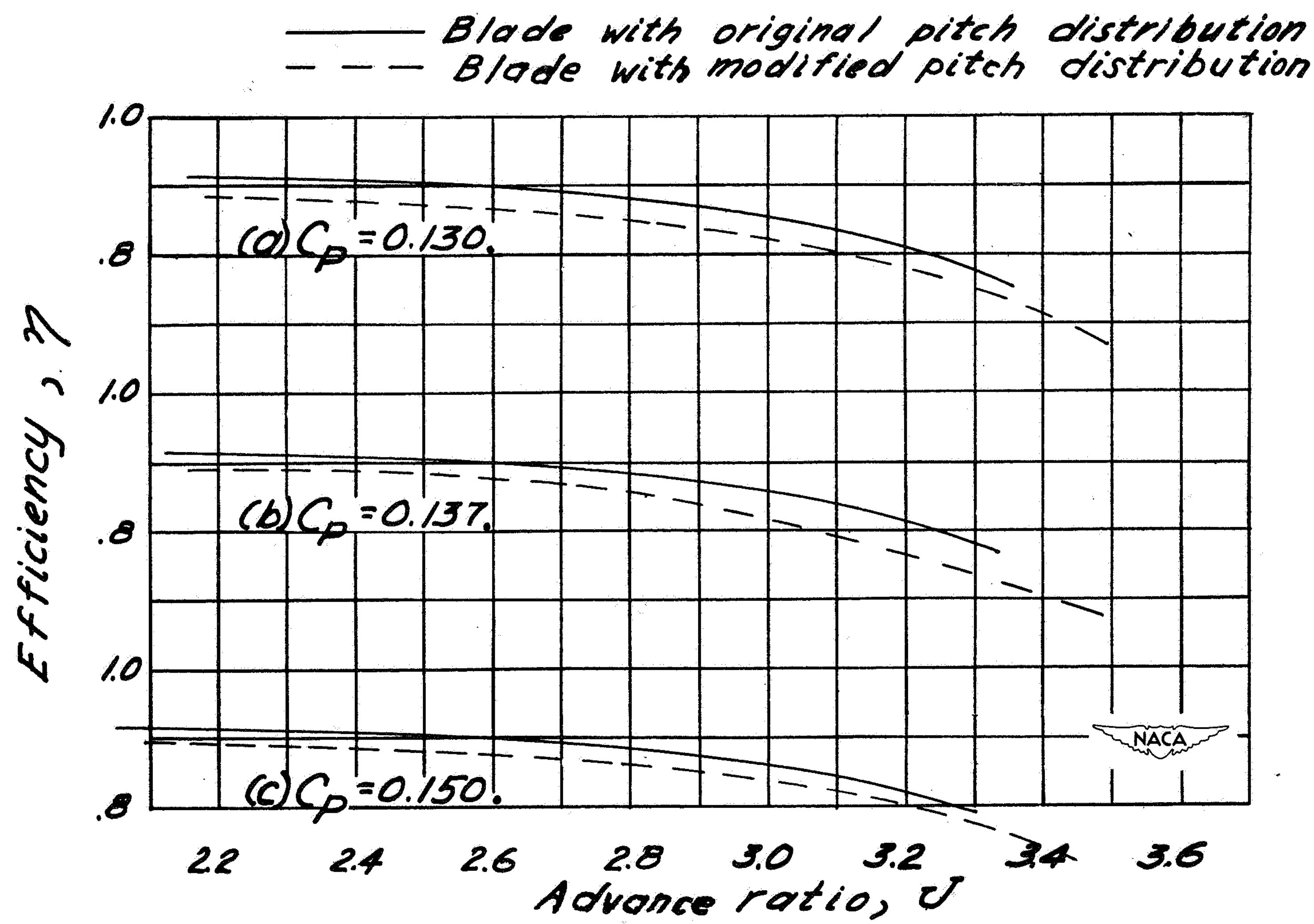

Figure 19.- Effect on efficiency of operation at constant power coefficient. $M_o = 0.20$.

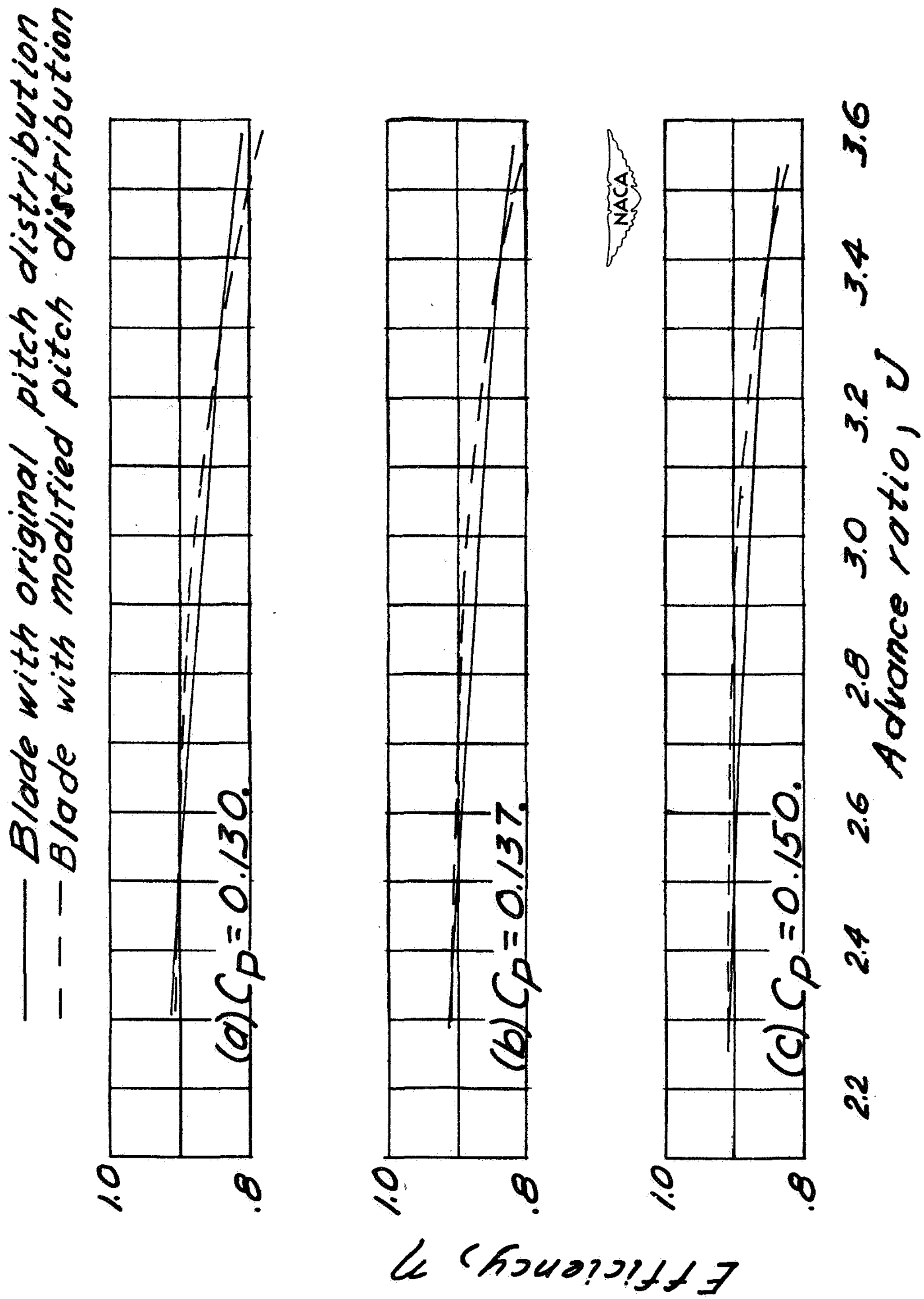

Figure 20.- Effect on efficiency of operation at constant power coefficient. $M_o = 0.53$.

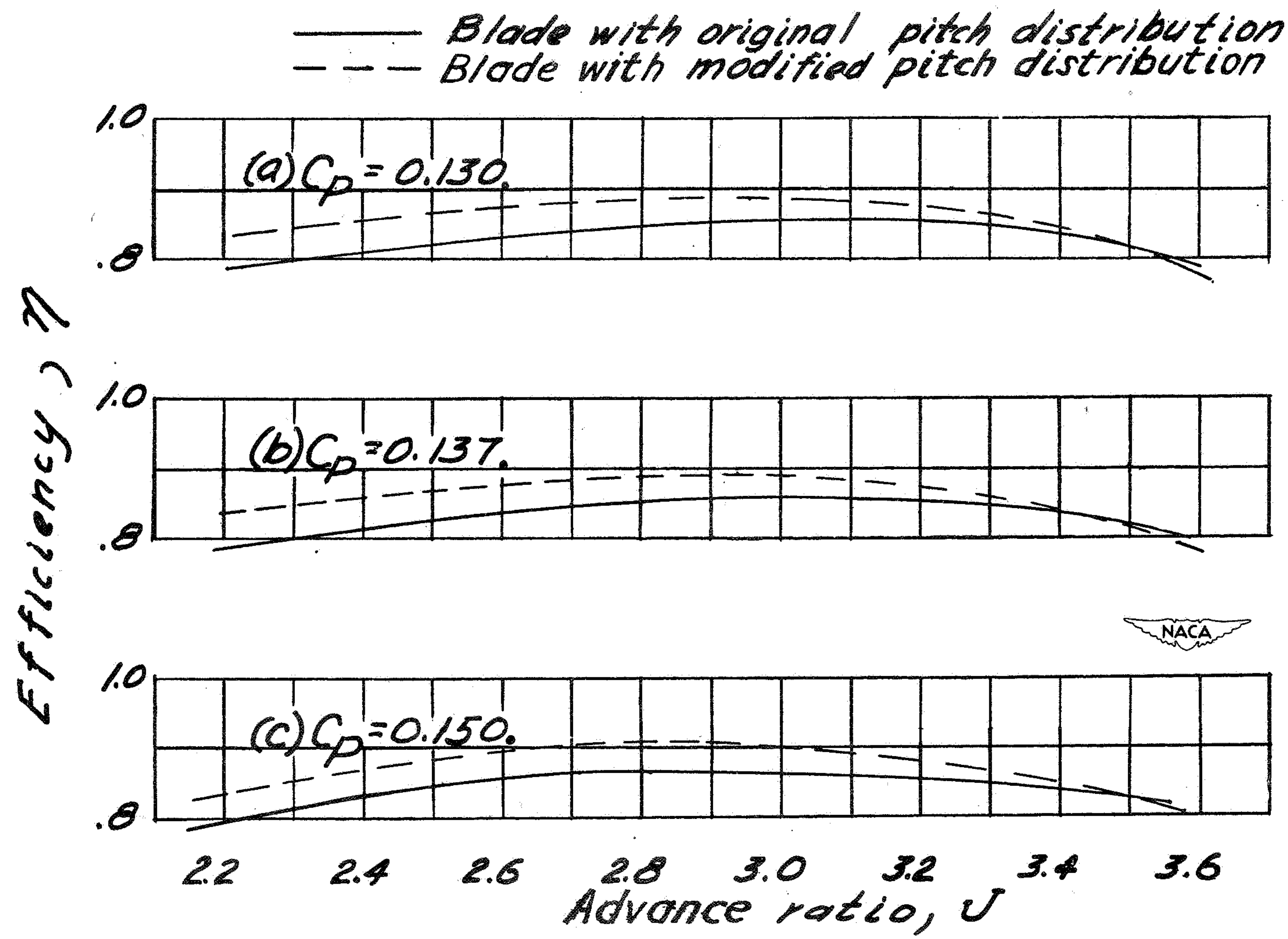

Figure 21.- Effect on efficiency of operation at constant power coefficient. $M_o = 0.62$.

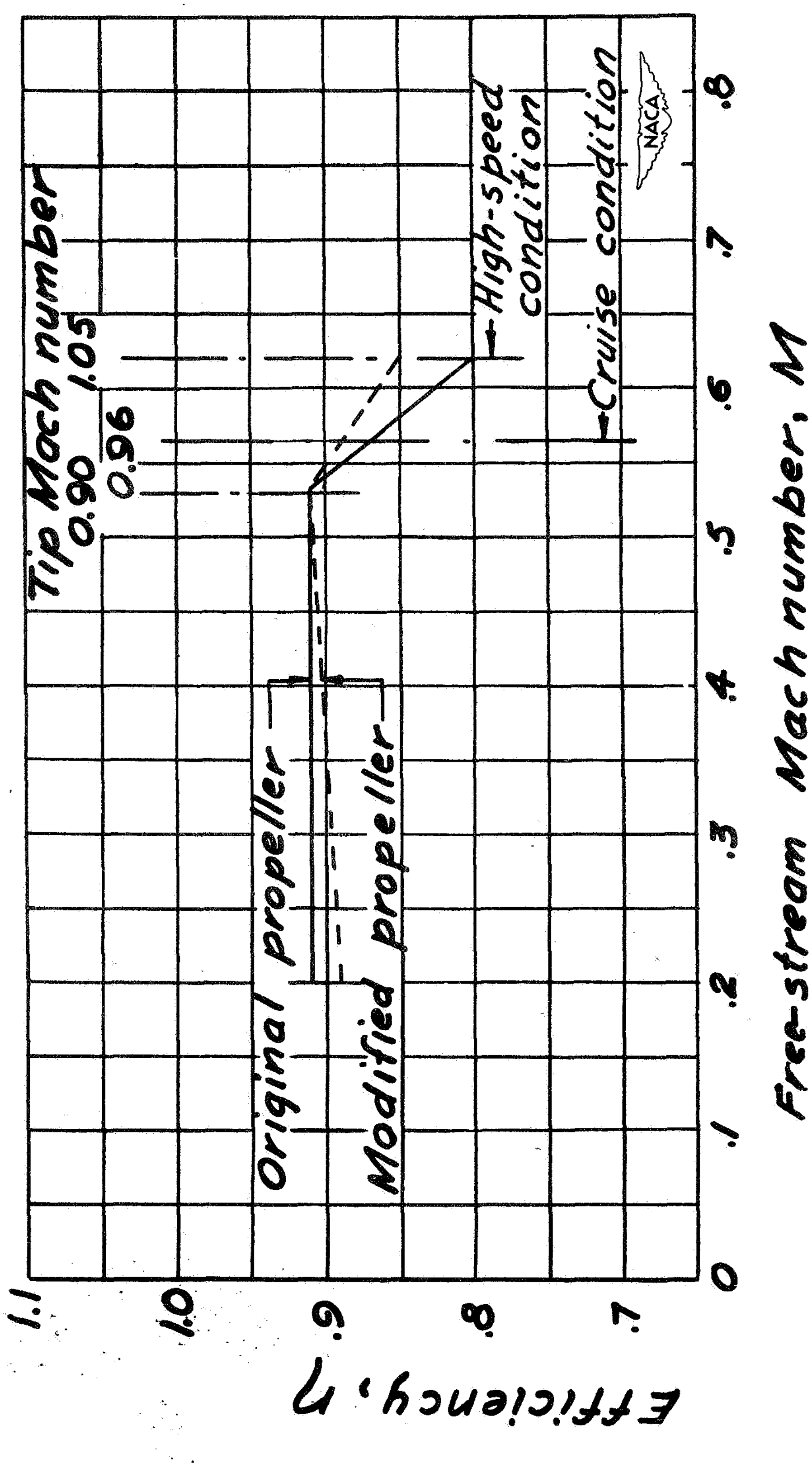

Figure 22.- Effect of compressibility on efficiency. $J = 2.30$; $C_P = 0.137$.

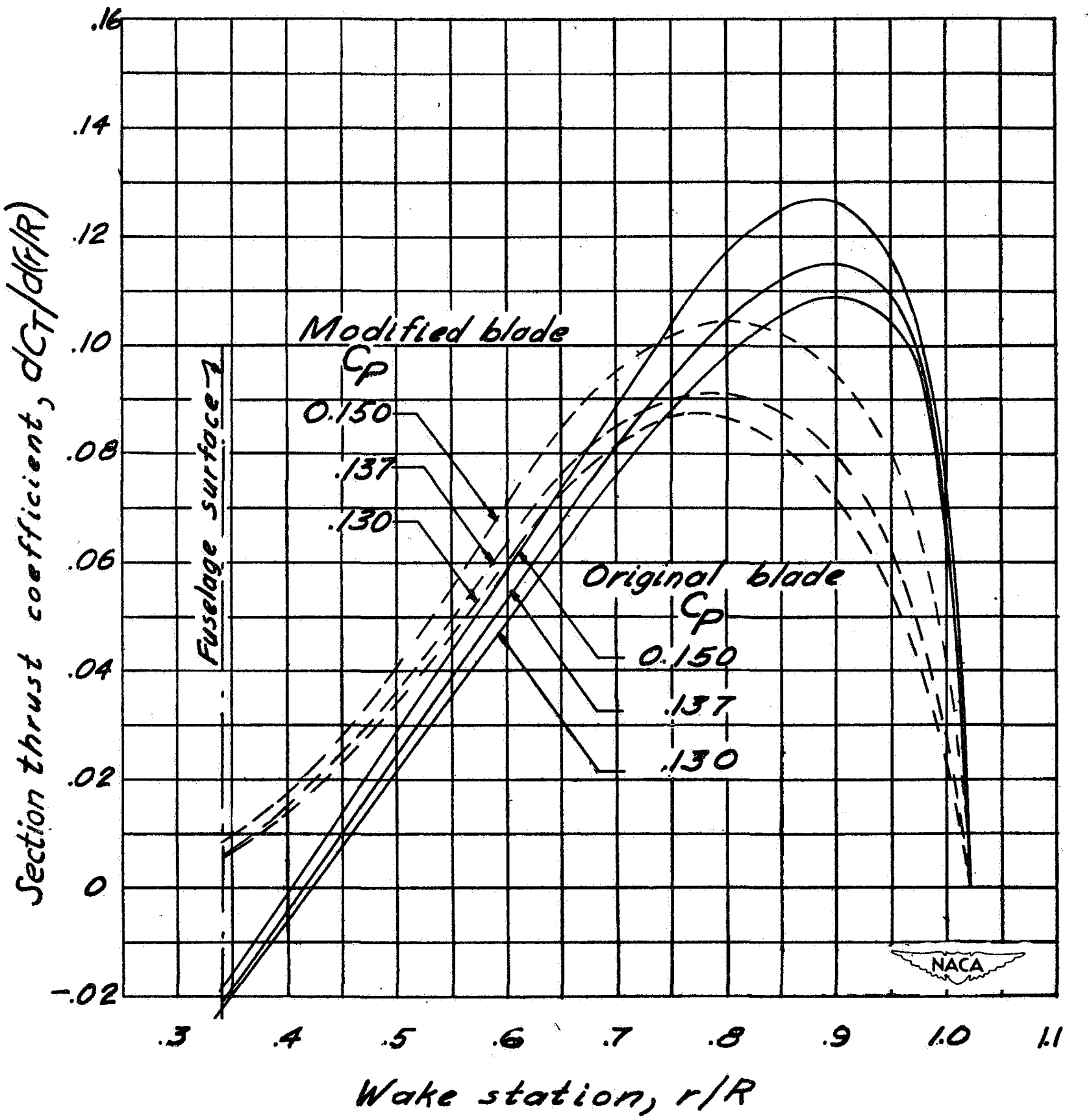

(a) $M_o = 0.53$.

Figure 23.- Comparison of section thrust-coefficient curves for constant power coefficients. J = 2.30.

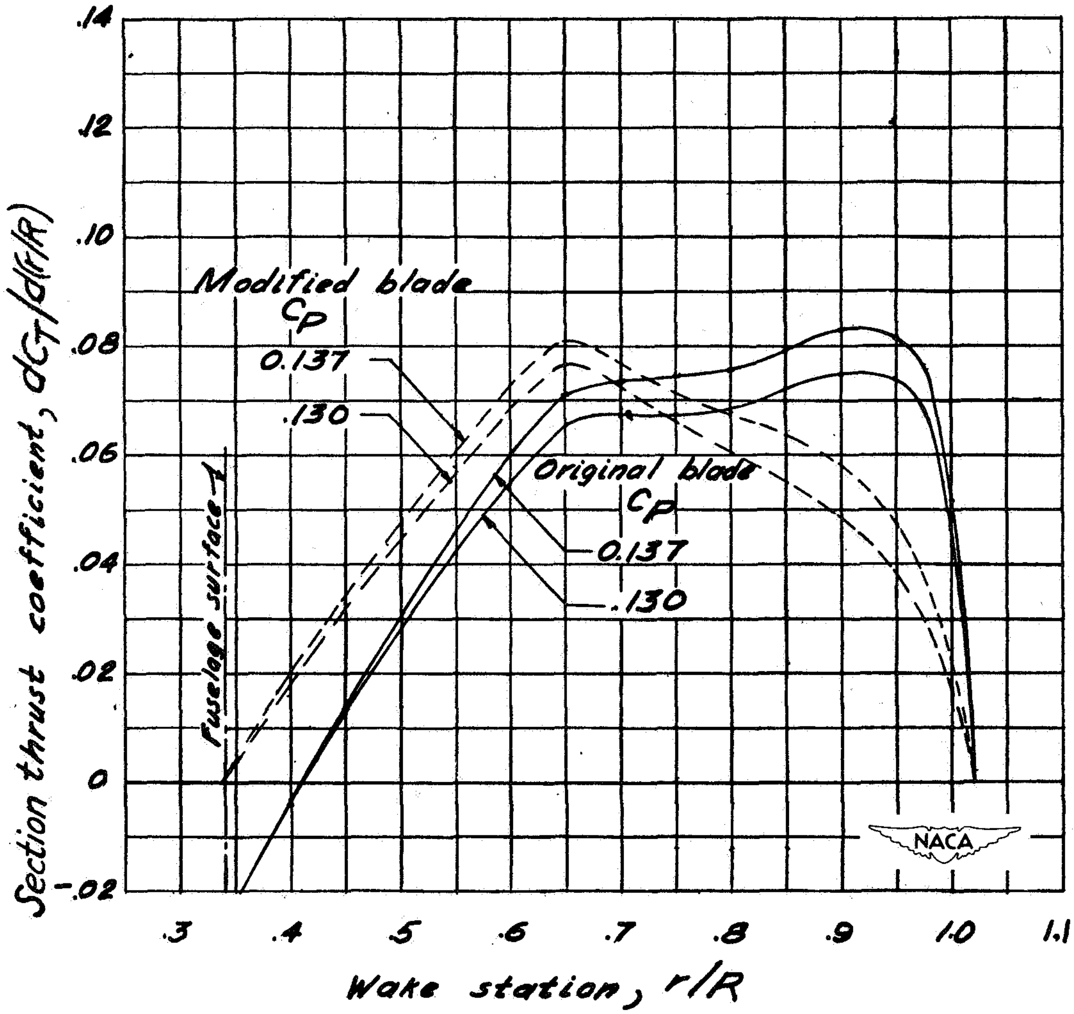

(b) $M_o = 0.62$.

Figure 23.- Concluded.

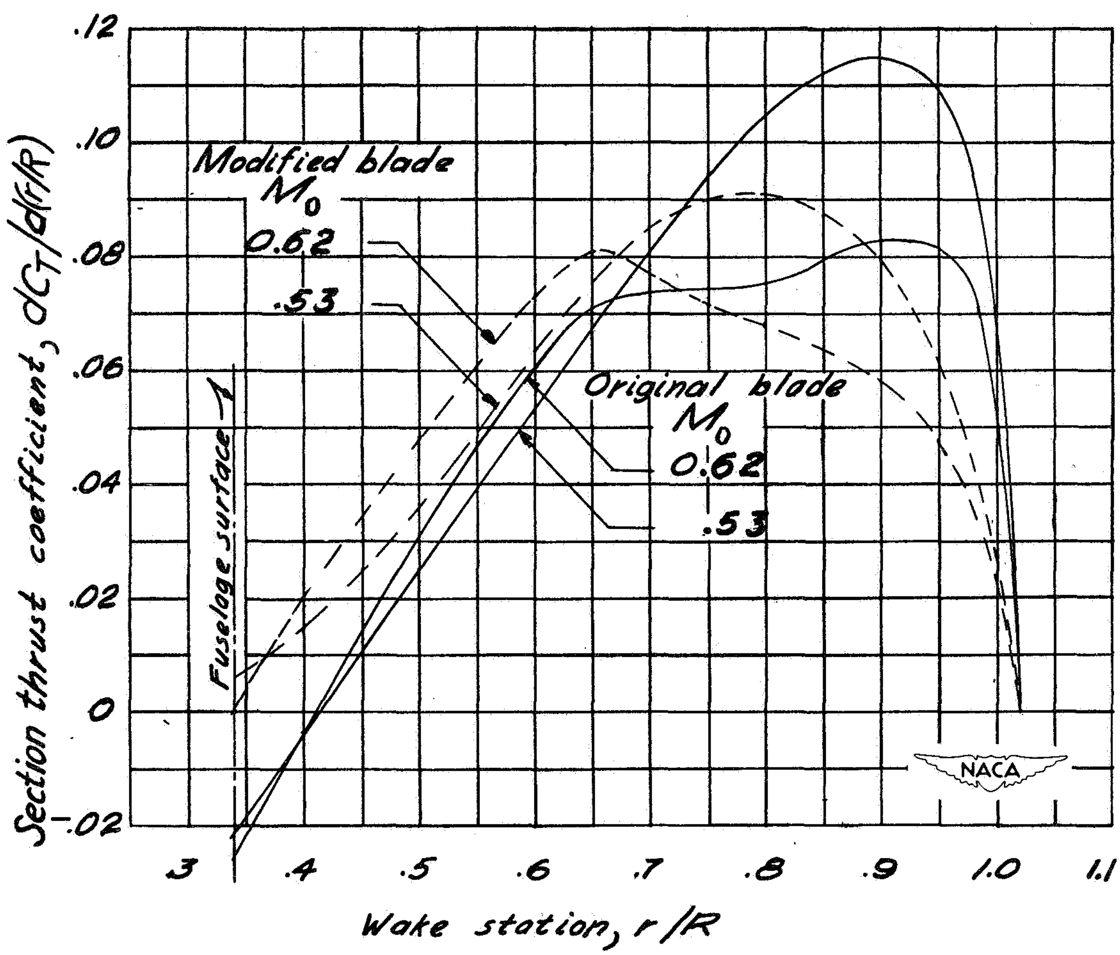

Figure 24.- Effect of compressibility on thrust distribution. J = 2.30; C_P = 0.137.

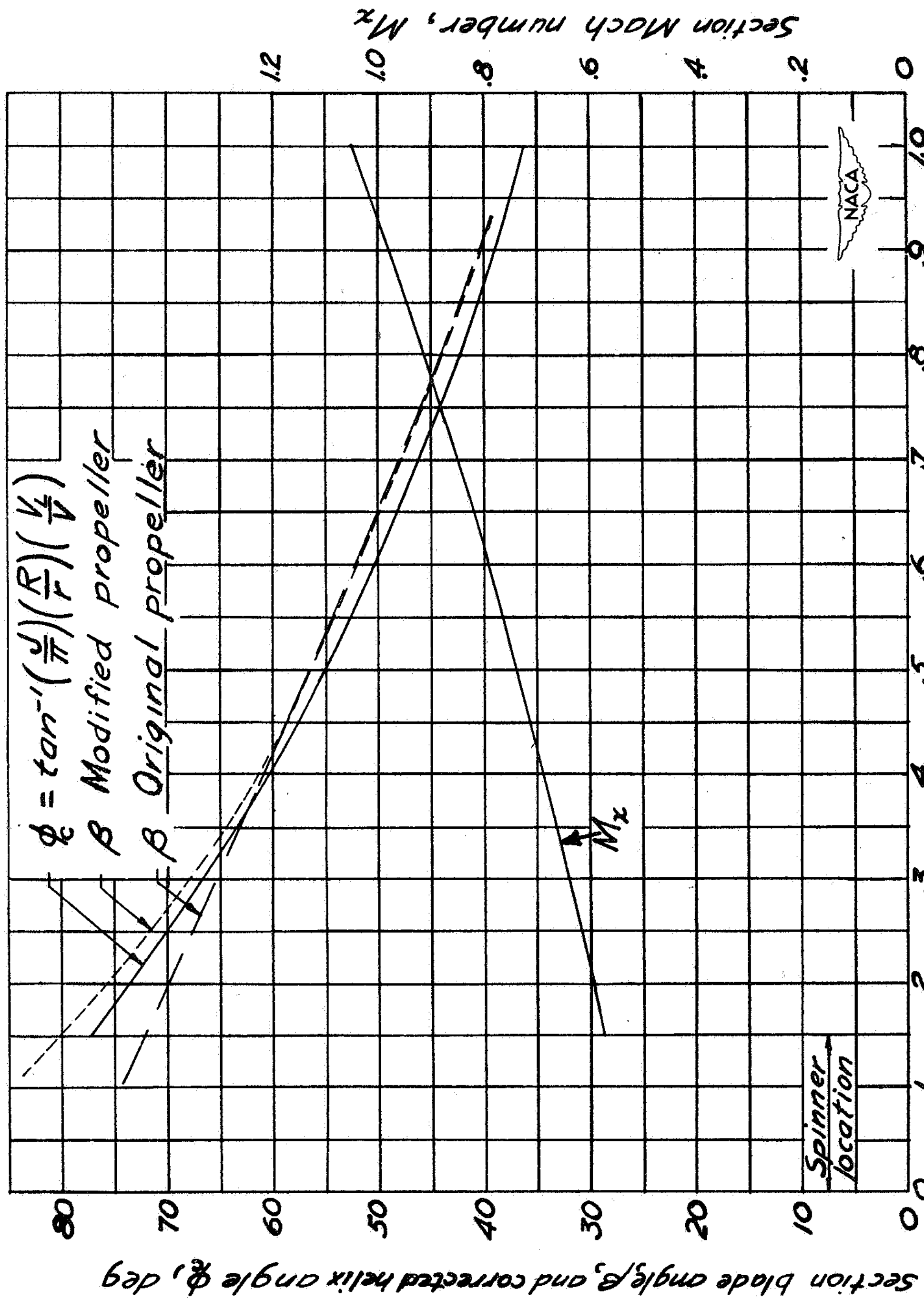

Figure 25.- High-speed operating condition. $M_o = 0.62$; $J = 2.30$; $C_P = 0.137$.